Journal of Biomolecular Structure and Dynamics





ISSN: (Print) (Online) Journal homepage: https://www.tandfonline.com/loi/tbsd20

Integrated gene expression profiling and functional enrichment analyses to discover biomarkers and pathways associated with Guillain-Barré syndrome and autism spectrum disorder to identify new therapeutic targets

Rizone Al Hasib, Md. Chayan Ali, Md Habibur Rahman, Sabbir Ahmed, Shaharin Sultana, Sadia Zannat Summa, Mst. Sharmin Sultana Shimu, Zinia Afrin & Mohammad Abu Hena Mostofa Jamal

To cite this article: Rizone Al Hasib, Md. Chayan Ali, Md Habibur Rahman, Sabbir Ahmed, Shaharin Sultana, Sadia Zannat Summa, Mst. Sharmin Sultana Shimu, Zinia Afrin & Mohammad Abu Hena Mostofa Jamal (29 Sep 2023): Integrated gene expression profiling and functional enrichment analyses to discover biomarkers and pathways associated with Guillain-Barré syndrome and autism spectrum disorder to identify new therapeutic targets, Journal of Biomolecular Structure and Dynamics, DOI: 10.1080/07391102.2023.2262586

To link to this article: https://doi.org/10.1080/07391102.2023.2262586

View supplementary material ☑	Published online: 29 Sep 2023.
Submit your article to this journal 🗷	Article views: 66
View related articles 🗹	View Crossmark data 🗷





Integrated gene expression profiling and functional enrichment analyses to discover biomarkers and pathways associated with Guillain-Barré syndrome and autism spectrum disorder to identify new therapeutic targets

Rizone Al Hasib^{a,b}, Md. Chayan Ali^{c*}, Md Habibur Rahman^{d,e}, Sabbir Ahmed^a, Shaharin Sultana^{a,b}, Sadia Zannat Summa^{a,b}, Mst. Sharmin Sultana Shimu^f, Zinia Afrin^a and Mohammad Abu Hena Mostofa Jamal^{a,b}

^aDepartment of Biotechnology and Genetic Engineering, Islamic University, Kushtia, Bangladesh; ^bLaboratory of Medical and Environmental Biotechnology Islamic University, Kushtia, Bangladesh; ^cDepartment of Biochemistry, The Netherlands Cancer Institute, Amsterdam, The Netherlands; ^dDepartment of Computer Science and Engineering, Islamic University, Kushtia, Bangladesh; ^eCenter for Advanced Bioinformatics and Artificial Intelligent Research, Islamic University, Kushtia, Bangladesh; ^fDepartment of Genetic Engineering and Biotechnology, University of Rajshahi, Rajshahi, Bangladesh

Communicated by Ramaswamy H. Sarma

ABSTRACT

Guillain-Barré syndrome (GBS) is one of the most prominent and acute immune-mediated peripheral neuropathy, while autism spectrum disorders (ASD) are a group of heterogeneous neurodevelopmental disorders. The complete mechanism regarding the neuropathophysiology of these disorders is still ambiguous. Even after recent breakthroughs in molecular biology, the link between GBS and ASD remains a mystery. Therefore, we have implemented well-established bioinformatic techniques to identify potential biomarkers and drug candidates for GBS and ASD. 17 common differentially expressed genes (DEGs) were identified for these two disorders, which later guided the rest of the research. Common genes identified the protein-protein interaction (PPI) network and pathways associated with both disorders. Based on the PPI network, the constructed hub gene and module analysis network determined two common DEGs, namely CXCL9 and CXCL10, which are vital in predicting the top drug candidates. Furthermore, coregulatory networks of TF-gene and TF-miRNA were built to detect the regulatory biomolecules. Among drug candidates, imatinib had the highest docking and MM-GBSA score with the well-known chemokine receptor CXCR3 and remained stable during the 100 ns molecular dynamics simulation validated by the principal component analysis and the dynamic cross-correlation map. This study predicted the gene-based disease network for GBS and ASD and suggested prospective drug candidates. However, more in-depth research is required for clinical validation.

KEY POINTS

- 17 common differentially expressed genes (DEGs) were identified from 693 DEGs of the GBS dataset (GSE72748) and 365 DEGs of the ASD dataset (GSE113834), which is the preliminary part of this investigation.
- From the PPI network analysis, a total of 10 hub genes were identified and two common DEGs named CXCL10 were found in both the hub gene and essential module analysis.
- The identified leading pathways and GO pathways, TF-gene interaction, and TF-miRNAs network has made the process more relevant and appropriate for suggesting probable drug candidates.
- Among the drug candidates, imatinib was suggested as the main drug candidate due to its interaction with the hub gene CXCL9 and CXCL10 and lower *p* value than the other candidates. It showed the highest binding affinity score and remained stable with the CXCR3 chemokine receptor.

ARTICLE HISTORY

Received 15 March 2023 Accepted 17 September 2023

KEYWORDS

Guillain-Barré syndrome; autism spectrum disorder; molecular docking; molecular dynamics simulation; principal component analysis; dynamic crosscorrelation map

1. Introduction

Guillain-Barré syndrome (GBS) is an inflammatory, acuteonset, immune-mediated peripheral nervous system disorder that has become the most prevalent contributor to neuromuscular paralysis (Berciano et al., 2017; Chang et al., 2012). GBS has significant residual morbidity (Bae et al., 2014) that worsens with age (0.06 per 100000 in infants and 2.07 per 100000 in older people aged 80 years or above), and males are considerably more prone to contract the disease than females (Webb et al., 2015). Although the specific reason behind the pathophysiology of GBS is not fully understood, it is believed that the condition has resulted from an adverse immune response to infections that affects the peripheral nerves (Leonhard et al., 2019). Before the onset of progressive muscle weakness, the majority of patients first exhibit

CONTACT Md Habibur Rahman Abib@iu.ac.bd; Mohammad Abu Hena Mostofa Jamal Jamalbtg@gmail.com
*Department of Molecular Biosciences, The University of Texas at Austin, 100 E. 24th St. Stop A5000, Austin, TX 78712, USA

⑤ Supplemental data for this article can be accessed online at https://doi.org/10.1080/07391102.2023.2262586.

This article was originally published with errors, which have now been corrected in the online version. Please see Correction (http://dx.doi.org/10.1080/07391102.2023.2262586)

an underlying disease, most often an upper respiratory tract infection (Shahrizaila et al., 2021). Various GBS outbreaks have been reported, most of which have been linked to infections with *Campylobacter jejuni*, while, other agents, like the Zika Virus (ZIKV), have also been closely connected (Anaya et al., 2017; Heikema et al., 2015). Based on the molecular mimicry of such infectious agents, they may react adversely with myelin or axonal parts of peripheral nerves, leading to various types of GBS (Ansar & Valadi, 2015; Dash et al., 2015).

In addition, the pathogenicity of GBS can be triggered by some key factors, such as immunization, trauma, bone-marrow transplantation, and surgery (Fujimura, 2013). Dysregulation and aberrant expression of several genes, particularly cytokine-coding genes, have previously been found in peripheral blood specimens retrieved from GBS patients while they undergo high-throughput expression profiling (Safa et al., 2021; Zhang et al., 2013). Although several earlier studies have shown links between particular genes and the prevalence of GBS (Blum et al., 2014, 2018), the specific mechanism underlying the genetic basis of GBS is still elusive (Barzegar et al., 2012).

Besides, autism spectrum disorder (ASD) is a neurodevelopmental disability defined by deficiencies in social and communication skills, speech difficulties, and repetitive behaviors that are assumed to be driven by abnormal neurotransmission mechanisms (Nisar et al., 2022). This prolonged neurodevelopmental condition exhibits both core and associated symptoms. Loss of social interactions and diffusive, stereotyped, and restricted behavior are the core symptoms of autistic people, while impatience, stress, violence, and various comorbidities are listed as associated symptoms (Bhandari et al., 2020). About 0.6 to 0.8% of people are estimated to be affected by ASD, while higher occurrences have also been observed (Christensen et al., 2016; Kim et al., 2011; Jussila et al., 2020). According to recent studies, approximately one in 36 children may have ASD, which has progressively increased in the past 20 years (Zablotsky et al., 2017). To date, no proper remedy is available for the core symptoms of ASD patients is available (Mostafavi & Gaitanis, 2020). Although there are considerable differences among patients with ASD, the disorder has a unique genetic link with a complex inheritance pattern (Lord et al., 2020; Veenstra-VanderWeele & Cook, 2004). Recent advances in the discovery of genes and genomic locations leading to ASD significantly enhance our understanding of the biology and major concerns necessary to clarify the pathophysiology of ASD (Manoli & State, 2021).

According to their breakthroughs in the regulation of disease molecular networks through multitargets on a systematic strategy, the pharmaceutical industry has recently prioritized omics-based polypharmacology due to the complexity of various diseases (Wang et al., 2012). The network pharmacological approach has drawn considerable attention since it combines system biology and genomics to reveal the interconnections between complex biological systems, drugs, and diseases (Sharma et al., 2022a; Sharma et al., 2022b). The discovery of disease-specific biomarkers and pharmacological

therapeutic targets has been accelerated by high-throughput methods based on '-omics' (Yang et al., 2020). Nowadays, high-throughput RNA sequencing has been used more extensively than gene expression microarray analysis in biological and drug research due to its shorter detection time and cost-effectiveness (Negi et al., 2022; Wang et al., 2009). However, the pathogenicity of GBS and ASD is not fully understood due to their complexity, and the study of the RNA-seq data for them has not been disclosed yet. Meanwhile, the link between GBS and ASD remains a mystery and no specific therapeutic strategy has developed in the last few decades.

Hence, we focused on identifying common differentially expressed genes and their subsequent biological pathways to explore the mysterious relationship between GBS and ASD. Two RNA sequencing datasets, GSE72748 (for GBS) and GSE113834 (for ASD), collected from GEO NCBI, were evaluated to identify differentially expressed genes. Based on common differentially expressed genes, the identification of gene ontology and identification of pathways, PPI analysis, hub genes and essential modules were accomplished. The identification of the hub gene from the PPI network was the core part of the study, as it facilitates the identification of probable drug candidates. Furthermore, TF-DEG interactions and TF-miRNA coregulatory network were also constructed to detect relevant transcription factors that regulate differentially expressed genes at the transcriptional level. The ultimate goal of this research was to find potential drug candidates for these two brain disorders. Finally, molecular docking, MM-GBSA calculation, density functional theory analysis, molecular dynamics simulation, principal component analysis (PCA), and dynamic cross-correlation mapping (DCCM) approaches were utilized to validate the potency of drug candidates (Figure 1).

2. Methodology

2.1. Collection of the dataset

We obtained the gene expression datasets for GBS and ASD from the GEO-NCBI database to examine the genetic relationship between them (Barrett et al., 2012). The accession number for the GBS dataset was GSE72748 (https://www. ncbi.nlm.nih.gov/geo/query/acc.cgi?acc=GSE72748) was obtained from peripheral blood mononuclear cells of a Guillain-Barré Syndrome patient and her healthy twin sampled at three distinct points of disease progression. The ASD dataset GSE113834 (https://www.ncbi.nlm.nih.gov/geo/ query/acc.cgi?acc=GSE113834) focused on comparing the expression of histamine-related genes in 13 patients with ASD and 39 matched controls. Both datasets use RNA-seq data and a high-throughput sequencing method was implemented for their expression profiling. For the GSE72748 dataset, the GPL10999 Illumina Genome Analyzer IIx platform (Homo sapiens) was used and GPL15207 [PrimeView] Affymetrix Human Gene Expression Array platform was used for the GSE113834 dataset. José de la Fuente et al. contributed to the GSE72748 dataset (Doncel-Pérez et al., 2016) and the GSE113834 dataset was provided by Parras et al. (2018).

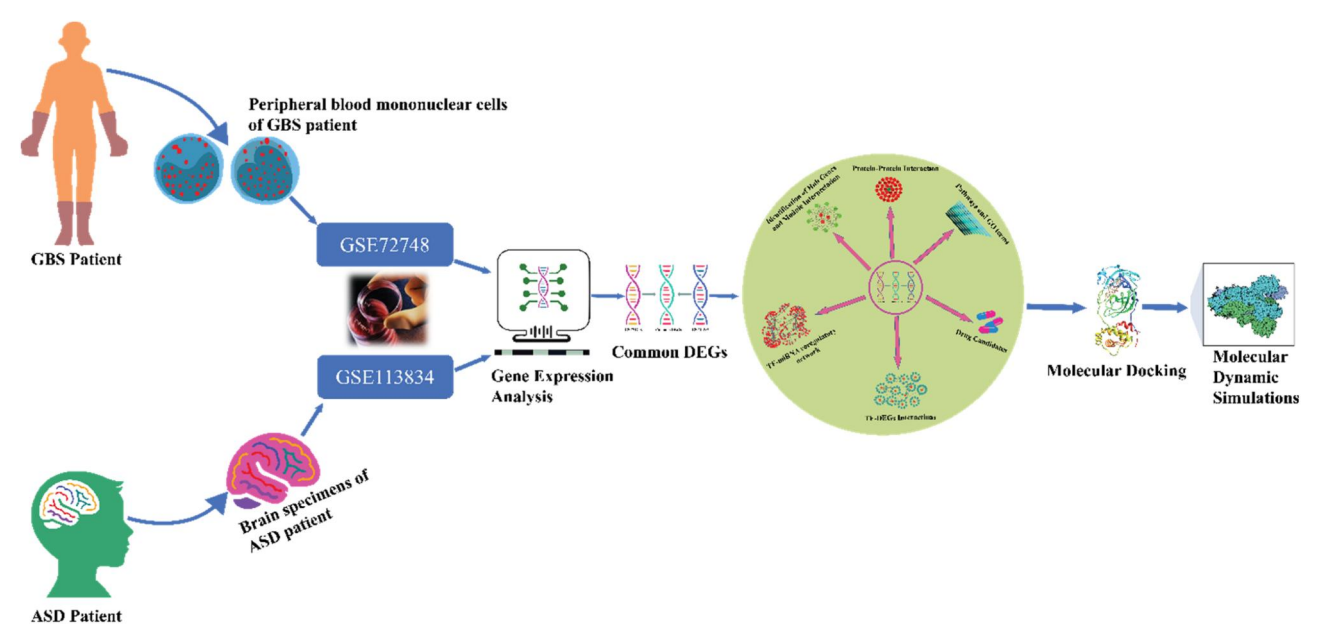


Figure 1. Graphical representation of the current study.

2.2. Identification of differentially expressed genes and common genes between GBS and ASD

The identification of differentially expressed genes (DEGs) is the key to determining the genetic connections between two diseases. In our study, we used the Bioconductor DESeg2 package in R to identify DEGs for GSE72748 and GSE113834 (Love et al., 2014). A threshold criterion, pvalue <0.05 and absolute log2 fold change (FC) > =1, was set for both datasets to identify the significant DEGs. Both datasets were normalized by log2 transformation before starting the analysis and the false discovery rate was managed by the Benjamini-Hochberg correction method (Benjamini Hochberg, 1995). Finally, using the programming language R, we locate the DEGs common to GSE72748 and GSE113834.

2.3. Identification of gene ontology and pathways by functional enrichment analysis

An enrichment analysis was carried out to identify gene ontological pathways and pathways for common DEGs via the web-based platform Enrichr (Kuleshov et al., 2016). Gene Ontology (GO) is a magnificent repository of computational information on the function of genes and their regulation (The Gene Ontology Consortium, 2017). We considered three categories, namely biological process, molecular function, and cellular component, for a better understanding of Gene Ontology (GO) (Doms & Schroeder, 2005). A pathway-based analysis maintains a high similarity to Gene Ontology (GO), but it offers more precise and detailed information on the molecular mechanisms that are responsible for complex diseases (Holmans et al., 2009; Tilford & Siemers, 2009; Wang et al., 2007). To identify significant pathways, we utilized three pathway databases: KEGG (Kanehisa et al., 2012), WikiPathways (Slenter et al., 2018), and BioPlanet (Huang et al., 2019).

2.4. Analysis of the PPIs network

Every protein is functionally interconnected with the other protein in the ribosomal complex (De Las Rivas & Fontanillo, 2010). Most proteins tend to trigger their functions through their interactions, and the retrieved PPI networks play a vital role in almost all biological processes (Athanasios et al., 2017). To build the PPI network of proteins encoded by common DEGs, we used the GeneMANIA database (http://www. genemania.org). GeneMANIA is a versatile and user-friendly web server for predicting gene functions by evaluating gene sets (Warde-Farley et al., 2010). In the PPI network, the proteins are represented by nodes, and their interactions are indicated by edges. PPI networks were analyzed using the Cytoscape app for better analysis and graphical visualization (Smoot et al., 2011). Cytoscape is a free software program that allows biologists to assess and interpret the interrelationship of a set of genes or proteins by visualizing, modeling, and analyzing molecular and genetic interaction networks (Yeung et al., 2008).

2.5. Identification of hub genes and Interpretation of essential modules

A hub gene is considered to be the protein in a PPI network that interacts with other proteins most frequently. To identify the hub genes, CytoHubba (http://apps.cytoscape.org/apps/ cytohubba), a Cytoscape plugin, was used in the current study. CytoHubba offers 11 topological analysis to identify significant nodes in biological networks and has become Cytoscape's most influential hub identification plugin due to its strong user-friendly interface (Chin et al., 2014). In addition, hub genes produce some highly dense areas in the protein-protein interaction network, which can be identified as the essential module. We used a Cytoscape plugin, Molecular Complex Detection (MCODE), to interpret the highly concentrated modules. Modules identified through

MCODE further contribute to the identification of potential drug candidates (Taz et al., 2021).

2.6. TF-DEGs interactions

We analyzed the associations between Transcription Factors (TFs) and common DEGs to identify regulatory biomolecules in terms of understanding the regulation of DEGs of interest at the transcriptional level. The online database NetworkAnalyst was utilized to investigate the TF-DEGs interaction (Xia et al., 2015). NetworkAnalyst is a powerful web server that enables its users to perform meta-analysis and differential expression analysis for single or multiple gene expression datasets (Xia et al., 2014; Zhou et al., 2019). The JASPAR database (https://jaspar.genereg.net/), available in NetworkAnalyst, was used for the topological analysis of the TF-DEGs interaction network.

2.7. Construction of the TF-miRNA coregulatory network

TF-miRNA coregulatory interactions were obtained from the RegNetwork database that helps to identify miRNAs and regulatory TFs at the transcriptional and post-transcriptional levels (Liu et al., 2015). NetworkAnalyst was used to visualize the TF-miRNA network and this platform enables researchers to explore big numbers of complex gene datasets for the generation of new biological hypotheses (Xia et al., 2015).

2.8. Identification of candidate drugs

The ultimate goal of our current study is the identification of drug molecules. We evaluate the common DEGs for GBS and ASD through the DSigDB database (Yoo et al., 2015) to identify candidate drugs. Access to the databases was obtained from the Enrichr online server. Enrichr is a user-friendly webbased platform that offers numerous forms of presentation summaries of collaborative gene functions for insightful enrichment analysis (Chen et al., 2013).

2.9. Homology modeling of the CXCR3 receptor

Using the Prime module in Schrodinger Maestro Suite (Jacobson et al., 2004), we accomplished the homology modeling of CXCR3. The UniProt database (https://www.uniprot. org/) was utilized to provide the human CXCR3 sequence (Accession ID: P49682). Due to the strong sequence resemblance, we chose the G protein-coupled CXCR2 structure of Homo sapiens (PDB ID: 6LFM) as the preferred template for homology modeling of human CXCR3 applying NCBI Protein BLAST against the PDB database. The alignment between the query and the selected template was calculated using the ClustalW alignment method. Finally, the knowledge-based model building method in Prime was applied to conduct the homology modeling. Then, the loop refinement and energy minimization of the built structure was performed using the OPLS3e force field in Schrodinger Prime. The minimized model was then validated using the Ramachandran plot, obtained from the PROCHECK web server (Laskowski et al., 2006).

2.10. Molecular docking and MM-GBSA calculation

Molecular docking is a drug discovery technique that can determine the interactions of amino acid residues between the target protein and prepared ligands in a conformation with the least amount of energy (Ferreira et al., 2015; Hasib et al., 2022). Here, we docked the top 10 identified drug molecules with the previously built CXCR3 receptor. The PubChem database was used to extract the 3D chemical structures of the identified drug molecules in SDF format. Then, the LigPrep module available in the Schrodinger Suite was used to prepare the ligands while maintaining the original state. Energy minimization was performed using the OPLS3e force field. The protein structure was prepared by the protein preparation wizard on the Maestro panel. During the preparation of the protein, hydrogen atoms were added and missing loops were also filled. Then, water molecules were removed within 3 Å of het groups and the structure was optimized. Finally, the OPLS3e force field was applied to minimize the structure of the protein. Further receptor grid boxes were generated using the 'Glide's Receptor Grid Generation' module at the active site of the receptor. The size of the grid box on the X, Y, and Z axis was 10 $\text{Å} \times 10$ $\hbox{\AA} imes$ 10 $\hbox{\AA}.$ Furthermore, we have calculated the MM-GBSA scores using the Prime module in Schrodinger Suite to justify the results of molecular docking (Campanella et al., 2008). Here, the OPLS3e force field and the VSGB 2.0 solvation model were utilized to perform the analysis (Roos et al., 2019; Li et al., 2011).

2.11. Density functional theory analysis for ligand optimization

The ligand was subjected to quantum mechanical optimization (QM) using density functional theory (DFT) calculations performed by Jaguar v-10.9 (Bochevarov et al., 2013). The DFT analysis employed B3LYP in combination with 6-31 G (d,p) basis sets. The ligand with the highest binding affinity and the MM-GBSA score was selected for DFT calculation. The analysis also focused on evaluating the frontier molecular orbitals, namely, the highest occupied molecular orbitals (HOMOs) and lowest unoccupied molecular orbitals (LUMOs), as well as their energy gap differences. The chemical hardness (η) and softness (S) can be determined using the following equations:

Hardness
$$(\eta) = (I - A)/2$$
 (1)

Softness (S) =
$$1/\eta$$
 (2)

In Equation (1), We represent the ionization potential (-EHOMO), while A denotes the electron affinity (-ELUMO). The lower the hardness value, the higher the reactivity, and vice versa. Softness (S) refers to an atom's ability to receive electrons, while η represents hardness.

2.12. Molecular dynamics simulation

A 100 ns molecular dynamics (MD) simulation of the proteinligand complex was performed to evaluate the binding stability of the drug compound to the CXCR3 receptor protein. The Schrodinger Desmond v3.6 program (https://www.schrodinger.com/), operating in a Linux environment, was employed to conduct the MD simulations and investigate the thermodynamic consistency of receptor-ligand complexes (Biswas et al., 2021). The TIP3P water solvation model was used in an orthorhombic simulation cell with periodic boundary condition at a separation distance of 10 Å (Harrach & Drossel, 2014). To achieve electrical neutralization, counter ions were used, and 0.15 M sodium chloride was added to simulate physiological conditions with 300K temperature and 1 atm pressure using NPT ensemble throughout the simulation period (Kandeel et al., 2023). The OPLS3e force field, available in the Desmond package, was used to minimize energy and relaxation of the system (Roos et al., 2019). Simulation snapshots were saved after 50 ps intervals. Molecular dynamics simulation snapshots were generated using the Schrödinger maestro application v9.5. The accuracy of the entire simulation event was assessed using the Simulation Interaction Diagram (SID) from the Desmond modules within the Schrodinger suite. The stability of the protein-ligand complex was ascertained by analyzing several factors such as root mean square deviation (RMSD), root mean square fluctuation (RMSF), solvent accessible surface area (SASA), the radius of gyration (Rg) and intramolecular hydrogen bonds values. Using the Bio3D package in R, the principal component analysis (PCA) and the dynamic crosscorrelation matrix (DCCM) were carried out.

2.13. MM-GBSA calculation from the molecular dynamics simulation trajectory

The binding free energy of ligands to macromolecules is commonly evaluated using the Molecular Mechanics Generalized Born Surface Area (MM-GBSA) methods (Genheden & Ryde, 2015). In this study, we employed the Prime module within the Schrodinger Maestro package to analyze the MM-GBSA calculation for the docked complex, based on the post-MD Simulations trajectory. The OPLS3e force field and the VSGB 2.0 solvation model were utilized to estimate the binding free energy. The total free energy binding was determined by the following equation:

$$dGbind = Gcomplex - (Gprotein + Gligand)$$

Here, dGbind represents the binding free energy, Gcomplex denotes the free energy of the complex, Gprotein corresponds to the free energy of the target protein, and Gligand represents the free energy of the ligand.

3. Results

3.1. Identification of differentially expressed genes and common genes between GBS and ASD

A total of 693 DEGs for Guillain-Barré syndrome (GBS) was identified from the GSE72748 dataset. Among them, 141 genes were up-regulated and 552 genes were down-regulated. The GSE102741 dataset was used for autism spectrum disorder (ASD) to identify DEGs. A total of 365 DEGs were identified where 92 genes were upregulated and 273 genes were downregulated. Cross-comparison analysis between 693 GBS genes and 365 ASD genes was done using the R programming language. We identified 17 (SNORA21, TNXB, SNORA61, CXCL9, CXCL10, HLA-L, CRISP3, TNFRSF12A, C1orf116, LOC100008587, PF4, CES1P1, C19orf33, HIST1H3D, LY6G5B, COL11A2, TMEM253) common DEGs for GBS and ASD through this approach. The overall results were represented by a Venn diagram and it revealed that, among the 1058 DEGs, 1.5% of genes are common (Figure 2).

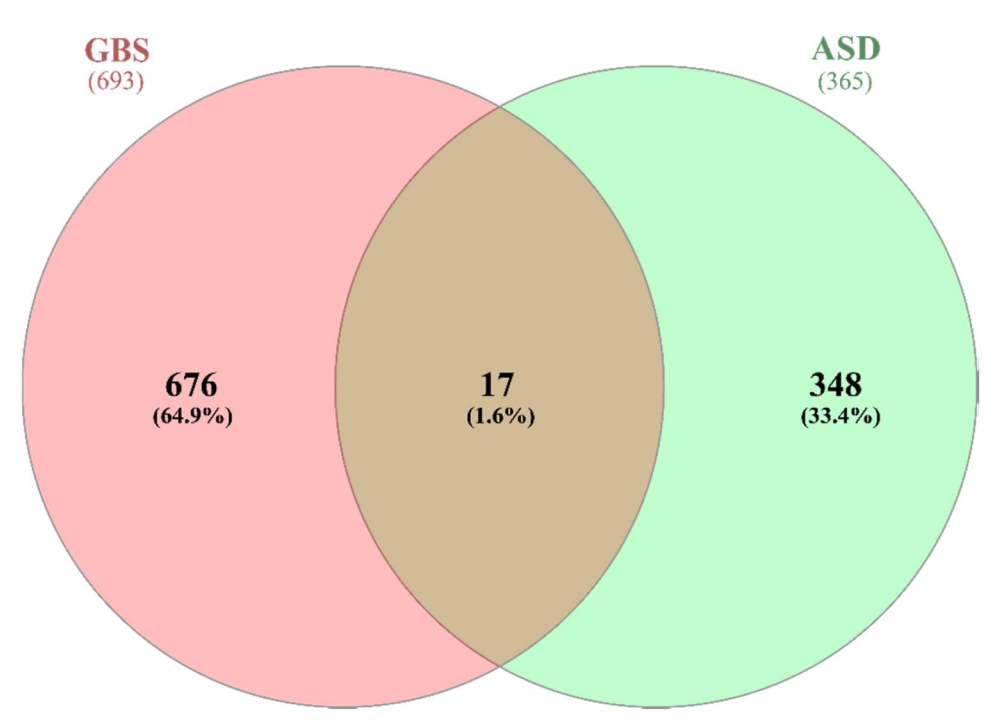


Figure 2. A Venn diagram for the representation of common differentially expressed genes. Among the 693 GBS DEGs and the 365 ASD DEGs, 17 DEGs are identical to both diseases, which is 1.6% of the total DEGs.

Table 1. Top three GO terms and their subsequent GO pathways with p values, combined scores, and corresponding DEGs.

GO terms	ID	GO pathways	p values	Combined scores	Genes
GO biological process	GO:0043950	Positive regulation of cAMP-mediated signaling	2.848E-08	14875.515	CXCL10, CXCL9, PF4
	GO:0030814	Regulation of cAMP metabolic process	1.451E-07	6739.106	CXCL10, CXCL9, PF4
	GO:1900544	Positive regulation of purine nucleotide metabolic process	1.845E-07	6032.529	CXCL10, CXCL9, PF4
	GO:0030801	Positive regulation of cyclic nucleotide metabolic process	2.836E-07	4962.477	CXCL10, CXCL9, PF4
	GO:0043949	Regulation of cAMP-mediated signaling	4.129E-07	4193.287	CXCL10, CXCL9, PF4
	GO:0030816	Positive regulation of cAMP metabolic process	1.310E-06	2518.932	CXCL10, CXCL9, PF4
	GO:0002688	Regulation of leukocyte chemotaxis	2.041E-06	2075.073	CXCL10, CXCL9, PF4
	GO:0002687	Positive regulation of leukocyte migration	3.002E-06	1753.749	CXCL10, CXCL9, PF4
	GO:0050921	Positive regulation of chemotaxis	8.615E-06	1107.217	CXCL10, CXCL9, PF4
	GO:0070098	Chemokine-mediated signaling pathway	1.106E-05	995.444	CXCL10, CXCL9, PF4
GO molecular function	GO:0045236	CXCR chemokine receptor binding	3.442E-07	4548.599	CXCL10, CXCL9, PF4
	GO:0008009	Chemokine activity	7.569E-06	1171.694	CXCL10, CXCL9, PF4
	GO:0042379	Chemokine receptor binding	9.172E-06	1077.273	CXCL10, CXCL9, PF4
	GO:0005125	Cytokine activity	2.866E-04	228.055	CXCL10, CXCL9, PF4
	GO:0008603	cAMP-dependent protein kinase regulator activity	0.0059356	1066.850	CXCL10
	GO:0004771	Sterol esterase activity	0.0076254	760.963	CES1P1
	GO:0004806	Triglyceride lipase activity	0.0210470	200.681	CES1P1
	GO:0016298	Lipase activity	0.0359419	98.691	CES1P1
	GO:0005178	Integrin binding	0.0769945	34.273	TNXB
	GO:0052689	Carboxylic ester hydrolase activity	0.0840661	30.164	CES1P1
GO cellular component	GO:0062023	Collagen-containing extracellular matrix	0.003796	62.11	TNXB, COL11A2, PF4
	GO:0034774	Secretory granule lumen	0.02894	29.59	CRISP3, PF4
	GO:1904724	Tertiary granule lumen	0.04575	71.15	CRISP3
	GO:0035580	Specific granule lumen	0.05143	60.57	CRISP3
	GO:0031093	Platelet alpha granule lumen	0.05547	54.54	PF4
	GO:0031091	Platelet alpha granule	0.07384	36.41	PF4
	GO:0042581	Specific granule	0.1277	16.04	CRISP3
	GO:0070820	Tertiary granule	0.1307	15.47	CRISP3
	GO:0070013	Intracellular organelle lumen	0.1608	5.51	CRISP3, COL11A2
	GO:0005788	Endoplasmic reticulum lumen	0.2166	6.63	COL11A2

3.2. Identification of gene ontology and pathways by functional enrichment analysis

To determine the relationship between different disorders, pathway-based research is needed because human diseases are interconnected with each other (Podder et al., 2020). We identified GO terms and significant signaling pathways for 17 common DEGs through the Enrichr web tool. For GO terms the top three subsections, namely biological process, molecular function, and cellular component, were evaluated, and for signaling pathway identification, we used Enrichr's KEGG, WikiPathways, and BioPlanet databases. Table 1 represents the top three GO terms (biological process, molecular functions, and cellular component) for the DEGs shared by GBS and ASD. The positive regulation of cAMP-mediated signaling and the regulation of the cAMP metabolic process were most profoundly regulated by the common DEGs in terms of GO biological process. GO molecular function disclosed the involvement of CXCR chemokine receptor binding and chemokine activity in common DEGs. For the GO cellular component, collagen-containing extracellular matrix and secretory granule lumen were highly involved in common DEGs. The results of KEGG, WikiPathways, and BioPlanet pathways are depicted in Table 2. In the case of the KEGG and WikiPathway, the chemokine signaling pathway and tolllike receptor signaling pathway were identified as the most interactive pathways along with the cytokine-cytokine receptor interaction and the type II interferon signaling pathway. Furthermore, the binding of chemokines to chemokine receptors, cytokine-cytokine receptor interaction, and TWEAK regulation of gene expression pathway were predominantly regulated by the common DEGs during the BioPlanet pathway analysis. Here, Figure 3(A) represented the bar graph for three GO terms, whereas Figure 3(B) showed the bar graph for the KEGG, WikiPathway, and Bioplanet pathway. For each category, only the top 10 relevant pathways were identified based on their lower pvalue.

3.3. Analysis of the PPI network

The functional interactions of proteins are predicted through the analysis of the PPI network which provides important aspects of disease analysis and drug design (Ayub et al., 2020; Miryala et al., 2018). In the current study, by importing all 17 common DEGs into the GeneMANIA database (https:// genemania.org/) as input data, we built a PPI network. Then, for better visual representation, the GeneMANIA network was reformed utilizing the Cytoscape app. The PPI network consists of 49 nodes and 781 edges, where each node is a single protein, and the protein interconnections are symbolized by the edges (Figure 4). This PPI network was later explored to detect the hub genes using different topological parameters to identify potential therapeutic targets.

3.4. Identification of hub genes and module interpretation for predicting therapeutic targets

The hub genes are the genes that exhibited the highest degree of connectivity in the principal module (Liu et al., 2020). Cytohubba plugin (Chen et al., 2009) from Cytoscape was used to identify hub genes based on their degree values. The top ten hub genes detected in our current study are CCL5, CCL18, CXCL12, CXCL1, CXCL8, CCL2, CCL2, CXCL9,

Table 2. Top 10 KEGG, WikiPathway, and BioPlanet pathways with their corresponding p values, combined scores, and interacting DEGs.

Terms	Pathways	p values	Combined scores	Genes
KEGG	Cytokine-cytokine receptor interaction	9.36E-05	193.823	CXCL10, CXCL9, TNFRSF12A, PF4
	Chemokine signaling pathway	5.20E-04	171.524	CXCL10, CXCL9, PF4
	Toll-like receptor signaling pathway	0.003	147.252	CXCL10, CXCL9
	Cytosolic DNA-sensing pathway	0.052	59.279	CXCL10
	RIG-I-like receptor signaling pathway	0.058	51.396	CXCL10
	ECM-receptor interaction	0.067	41.399	TNXB
	Protein digestion and absorption	0.074	36.406	COL11A2
	IL-17 signaling pathway	0.076	34.787	CXCL10
	TNF signaling pathway	0.090	27.500	CXCL10
	Systemic lupus erythematosus	0.107	20.982	HIST1H3D
WikiPathway	Chemokine signaling pathway	3.38E-04	210.839	CXCL10, CXCL9, PF4
•	Type II interferon signaling	4.45E-04	586.461	CXCL10, CXCL9
	Toll-like Receptor Signaling Pathway	0.003	149.214	CXCL10, CXCL9
	Regulation of toll-like receptor signaling pathway	0.006	98.524	CXCL10, CXCL9
	Platelet-mediated interactions with vascular and circulating cells	0.014	330.974	PF4
	miRNA targets in ECM and membrane receptors		236.908	TNXB
	Hippo-Yap signaling pathway		223.630	CXCL10
Focal Adhesion-PI3K-Akt-mTOR-signaling pathway		0.027	31.562	TNXB, COL11A2
The effect of progerin on the involved genes in Hutchinson-Gilfo Progeria Syndrome		0.031	120.296	HIST1H3D
	Fibrin Complement Receptor 3 Signaling Pathway	0.031	120.296	CXCL10
BioPlanet	Binding of chemokines to chemokine receptors	1.23E-05	946.732	CXCL10, CXCL9, PF4
	Cytokine-cytokine receptor interaction	6.26E-05	225.034	CXCL10, CXCL9, TNFRSF12A, PF4
	TWEAK regulation of gene expression	2.36E-04	889.102	CXCL10, TNFRSF12A
	Chemokine signaling pathway	5.12E-04	172.806	CXCL10, CXCL9, PF4
	Peptide G-protein coupled receptors	5.36E-04	169.007	CXCL10, CXCL9, PF4
	G alpha (i) signaling events	5.95E-04	160.657	CXCL10, CXCL9, PF4
	Type II interferon signaling (interferon-gamma)	8.13E-04	393.962	CXCL10, CXCL9
	ECM-receptor interaction	0.002	196.926	TNXB, COL11A2
	Thymic stromal lymphopoietin (TSLP) pathway	0.003	179.351	CXCL10, CXCL9
	GPCR ligand binding	0.005	55.255	CXCL10, CXCL9, PF4

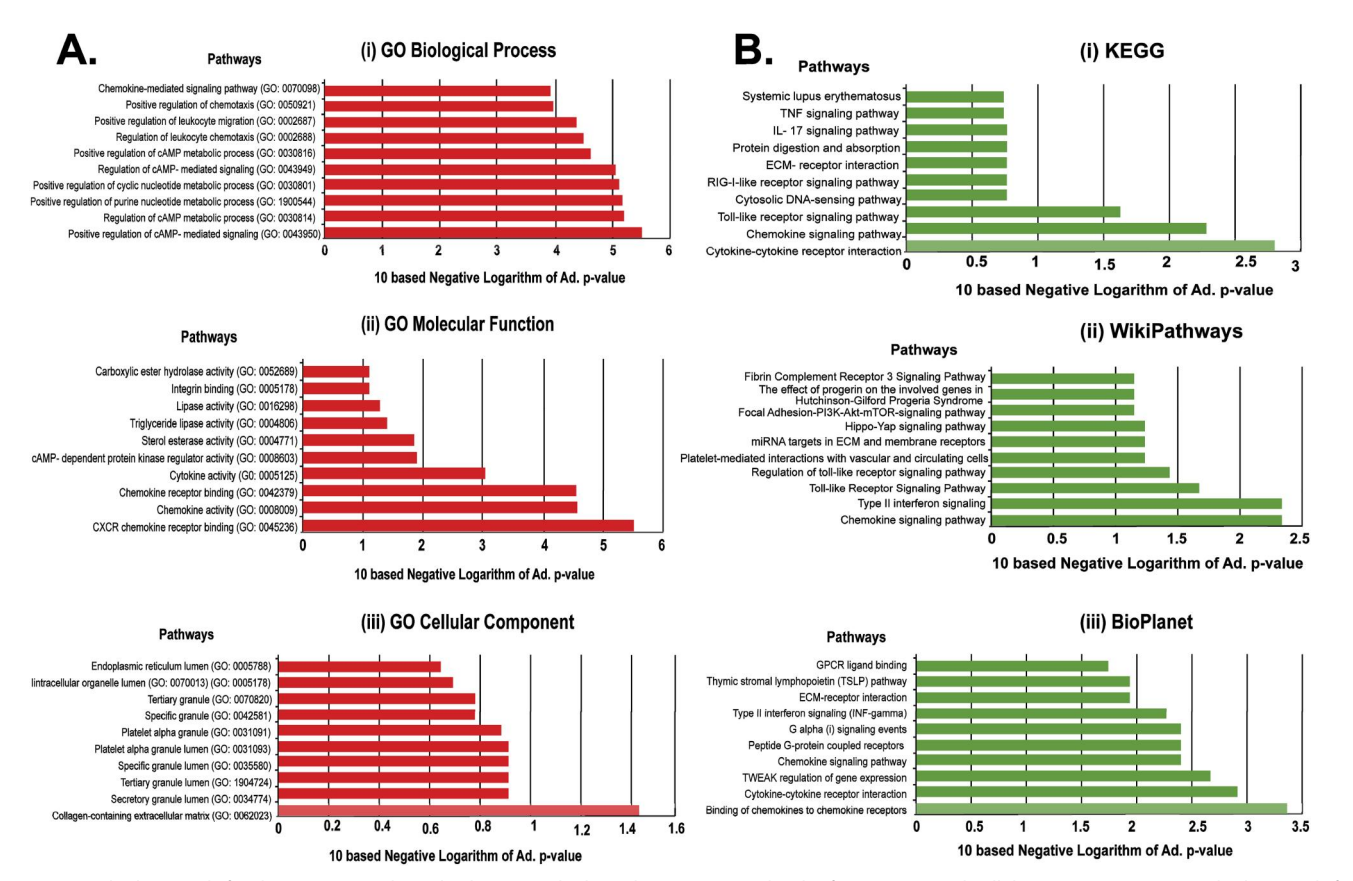


Figure 3. (A) the bar graph for three gene ontological subsections, biological process (i), molecular function (ii), and cellular component (iii). (B) The bar graph for (i) KEGG, (ii) WikiPathway, and (iii) BioPlanet. The top 10 pathways for each term were identified based on their lower pvalue.

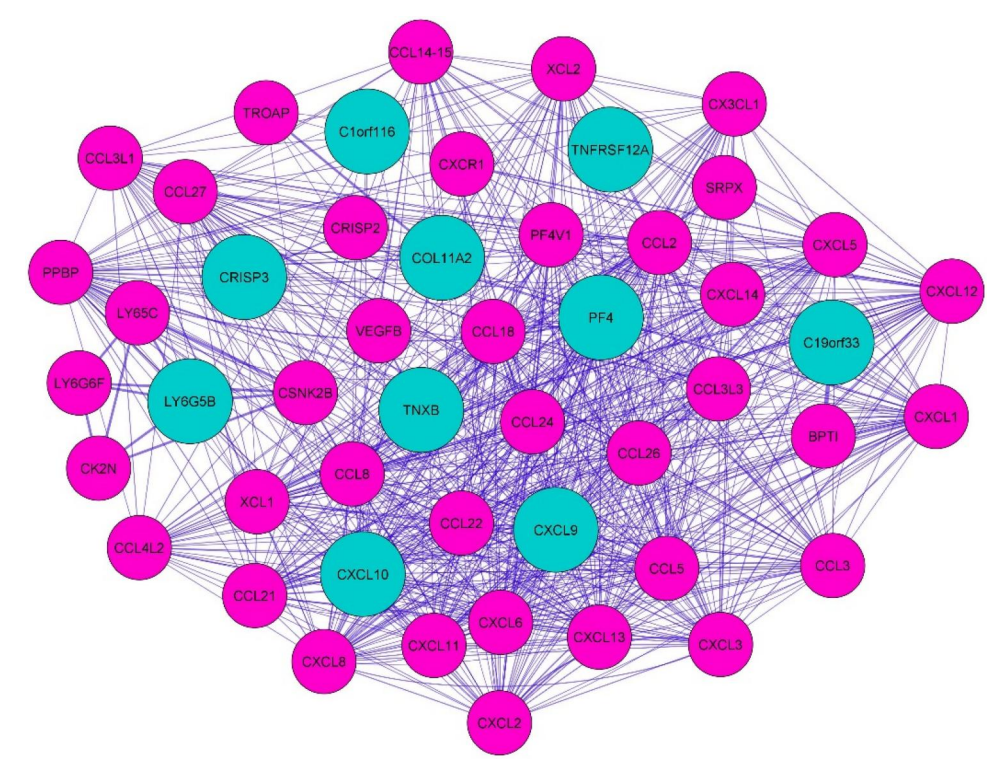


Figure 4. The protein-protein interaction network for common DEGs. The network consists of 49 nodes and 781 edges. Each node represents the differentially expressed genes, and the edges indicate the link between the genes. The nodes in cyan specify the common differentially expressed genes.

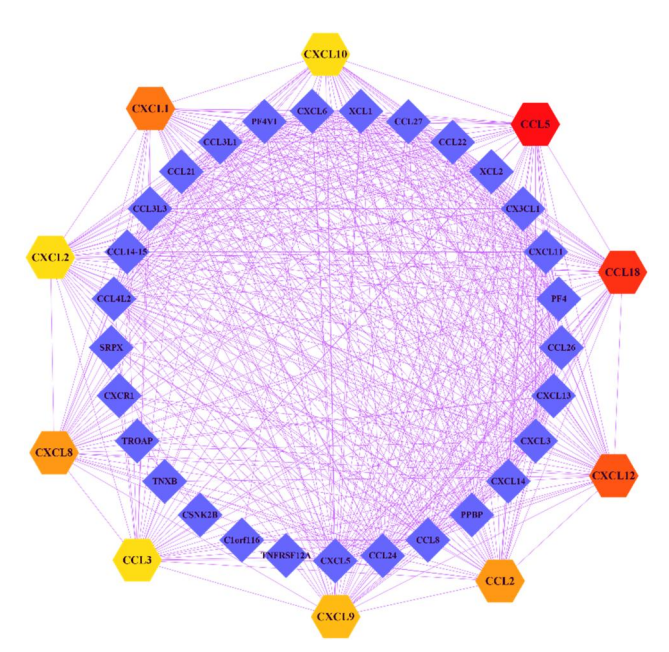


Figure 5. Identification of hub genes from the protein-protein interaction network. The network contains 39 nodes and 522 edges where the highlighted nodes indicate the hub genes. In this interactive network, CCL5 exhibited the highest degree value of 66.

CXCL10, CXCL2, and CCL3. The protein-protein interaction network for hub proteins and other correlated proteins was demonstrated in Figure 5. The interacting network has 39 nodes and 522 edges. These identified hub genes may be used as potential drugs in the future.

Furthermore, the results of different topological parameters for hub genes are shown in Table 3. Next, the highly connected module analysis was done using another

Table 3. Topological parameters including degree, closeness centrality, eccentricity, and clustering coefficient for 10 hub genes.

Hub genes	Degree	Closeness centrality	Eccentricity	Clustering coefficient
CCL5	66	38.66667	0.33333	0.30583
CCL18	62	39.33333	0.33333	0.35272
CXCL12	60	40.83333	0.33333	0.38588
CXCL1	59	39.16667	0.33333	0.39158
CXCL8	58	38.66667	0.33333	0.40169
CCL2	58	39.83333	0.33333	0.40653
CXCL9	54	38.66667	0.33333	0.46681
CXCL10	52	39.16667	0.33333	0.50679
CXCL2	52	40.83333	0.33333	0.51735
CCL3	52	39.16667	0.33333	0.51056

Cytoscape plugin named MCODE. The functional module derived from the PPI network plays an important role In controlling a specific cellular process (Li et al., 2012). In our study, the module analysis network contains 32 nodes and 671 edges, demonstrating that common DEGs CXCL9, CXCL10, and PF4 were highly interconnected in the dense module network (Figure 6).

3.5. TF-gene interactions

In cellular processes, TFs play a pivotal role and control gene expression in all living organisms at the transcriptional level (Cheng et al., 2012). We analyzed TF-gene interactions for the common DEGs through the NetworkAnalyst online database. The TFs-DEGs network was shown in Figure 7, which revealed that the network comprises 87 nodes and 138 edges, of which 72 TF-genes were found. In this network, each TF-gene regulates at least one common differentially expressed gene, among them, TNXB was regulated by the highest number of TF-genes (57 TF-genes).

3.6. TF-miRNA coregulatory network

miRNAs are short, single-stranded noncoding RNAs that participated in the regulation of gene expression at the posttranscriptional level (Cao et al., 2016), miRNAs have a pivotal role as a biological regulator in neurodegenerative disorders such as neuronal differentiation, neurogenesis, and synaptic plasticity (Rahman et al., 2020). Therefore,

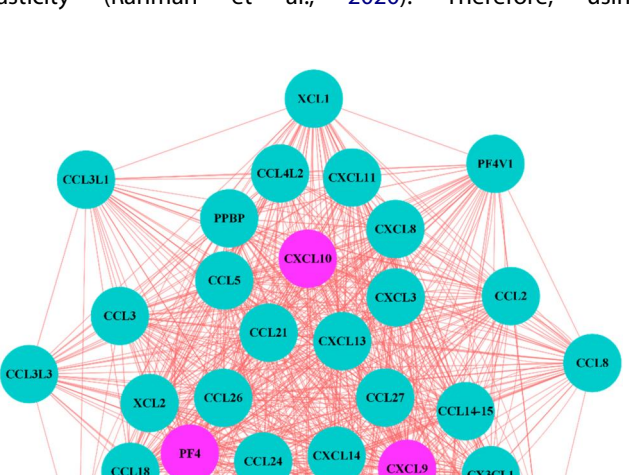


Figure 6. Essential module interpretation network generated from the PPI network. This network contains 32 nodes and 671 edges in which CXCL9, CXCL10, and PF4 were marked pink because these three hub genes are common in both the GBS and ASD datasets.

NetworkAnalyst, we constructed the TF-miRNA coregulatory network to obtain detailed information on these regulatory biomolecules that regulate our common DEGs. The TFmiRNA coregulatory network contains 177 nodes and 218 edges, of which 85 miRNAs and 79 TF-genes were identified. These identified TF-genes and miRNAs highly interacted with our common DEGs (Figure 8).

3.7. Identification of candidate drugs

Based on the lower pvalue and adjusted pvalue, the top 10 drug molecules for 17 common DEGs were identified from the DSigDB database of the Enrichr web server. The drug candidates that had a lower pvalue and adjusted pvalue, and linked with the hub genes CXCL9 and CXCL10 were considered for further evaluation. According to our experiment, these two hub genes were identified as dense modules and were closely related to each analysis of the study. Therefore, these two common nodes were emphasized over the other DEGs to identify candidate drugs.

The result obtained from the database revealed that Gadodiamide hydrate CTD 00002623 and Imatinib CTD 00003267 exhibited lower pvalue and adjusted pvalue compared to the rest of the drug candidates. Most drug candidates including these two molecules were found to be associated with CXCL9 and CXCL10 in the following study. Table 4 represents the top 10 drug candidates detected from DSiaDB.

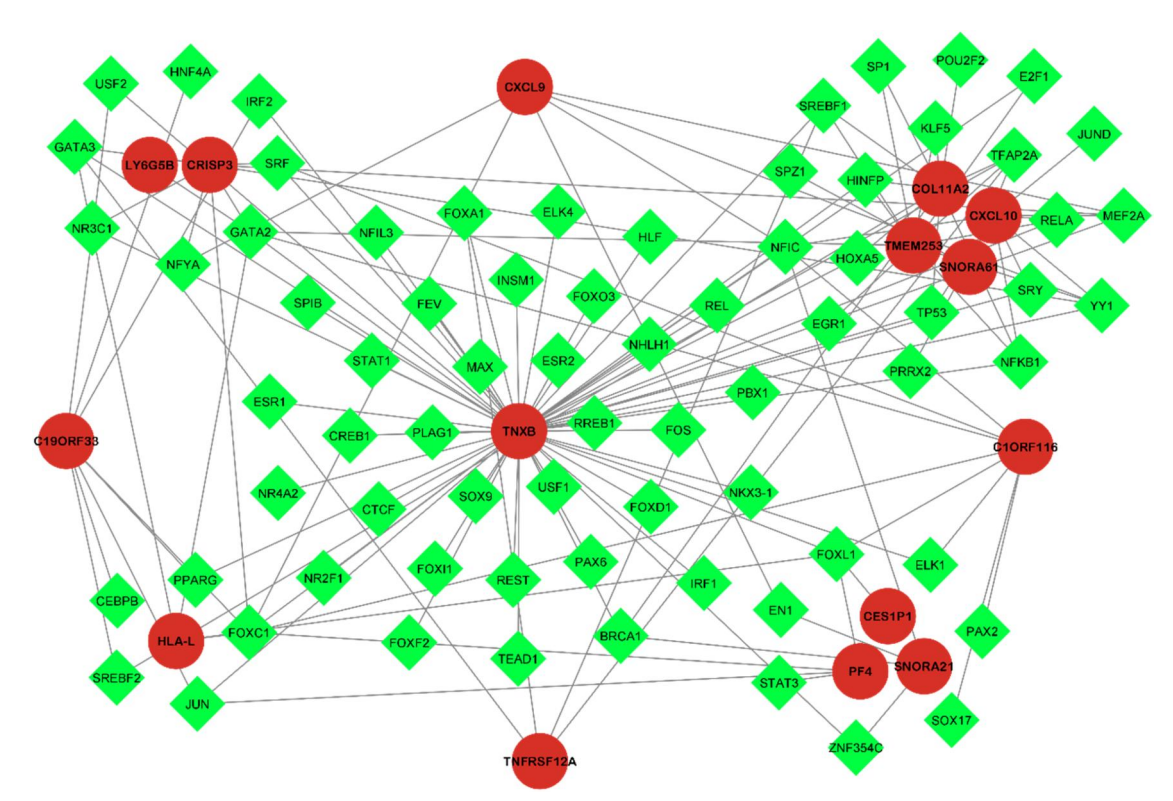


Figure 7. The TF-gene interaction network. This network has 87 nodes and 138 edges where 72 genes were determined as TF-genes. The nodes in maroon color indicate the common differentially expressed genes.

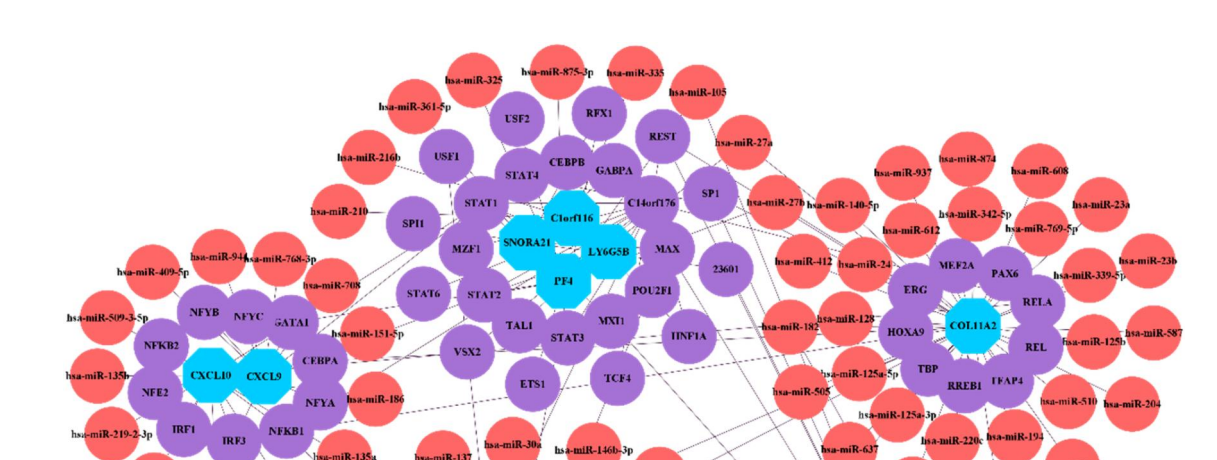


Figure 8. Representation of the TF-miRNA coregulatory network. The network holds 177 nodes and 218 edges in which 85 miRNAs and 79 TF-genes were present. The nodes in the cyan color represent the common DEGs, the nodes in the maroon color are miRNAs, and the purple nodes specify the TF-genes.

Table 4. Top 10 suggested drug molecules for GBS and ASD with their pyalue, adjusted pyalue, and interacting DEGs.

Drug candidates	p value	Adjusted p value	Interacting genes
Gadodiamide hydrate CTD 00002623	6.02E-04	0.20049641	CXCL10, CXCL9
Imatinib CTD 00003267	0.003527	0.20049641	CXCL10, CXCL9
Cicloheximide PC3 UP	0.00374	0.20049641	C10RF116, TNFRSF12A, HIST1H3D
Thapsigargin PC3 UP	0.007439	0.20049641	C10RF116, TNFRSF12A, HIST1H3D
Irinotecan PC3 UP	0.008179	0.20049641	C1ORF116, SNORA21, HIST1H3D
Lycorine PC3 UP	0.008496	0.20049641	C10RF116, TNFRSF12A, HIST1H3D
3-Nitrofluoranthene CTD 00001617	0.010155	0.20049641	CXCL10
Roxarsone CTD 00006708	0.010997	0.20049641	CXCL9
Roflumilast CTD 00003916	0.010997	0.20049641	CXCL10
Rolipram CTD 00007371	0.012679	0.20049641	CXCL10

3.8. Protein modeling, molecular docking, and MM-GBSA analysis

The homology modeling, refinement, and energy minimization of the 3D structure of CXCR3 receptor protein (Figure 9(A)) was carried out by the Prime module of the Schrodinger Suite (paid version). Structural validation of the built protein was performed by the Ramachandran plot. The modeled protein had 368 amino acid residues, where 91.8% of the residues fall into the most favoured regions (residues in the red zone of Figure 9(B-i)). Almost similar results have been observed when the ligand imatinib binds to the CXCR3 receptor (Figure 9(B-ii)). 90.03% of the residues were present in the most favoured regions in the case of receptor-ligand binding.

The energy of the ligand-receptor binding was then calculated by the molecular docking approach as it is most

extensively utilized in drug discovery to interpret the ligand-target interaction and identify possible therapeutic target compounds (Pinzi & Rastelli, 2019). In our study, we docked the top 10 drug molecules that were identified from the DSigDB database to gain more information on their interaction with the CXCR3 receptor.

The results revealed that imatinib exhibited the highest binding affinity of -7.338 kcal/mol. Imatinib interacted with A: TYR-270 by forming a hydrogen bond and with A: PHE-46,130 by a pi-pi stacking bond (Figure 10). in addition, imatinib interacted with A: GLU-292 through a salt-bridge bond and formed a pi-cation bond to interact with A: LYS-299 (Figure 10). to validate the results of molecular docking analysis, we calculated the MM-GBSA values of the top 10 drug molecules. Complying the molecular docking, imatinib exhibited the highest MM-GBSA score of -68.27 kcal/mol. Table 5 represents the binding affinity and MM-GBSA scores for the top 10 drug molecules. Thereafter,

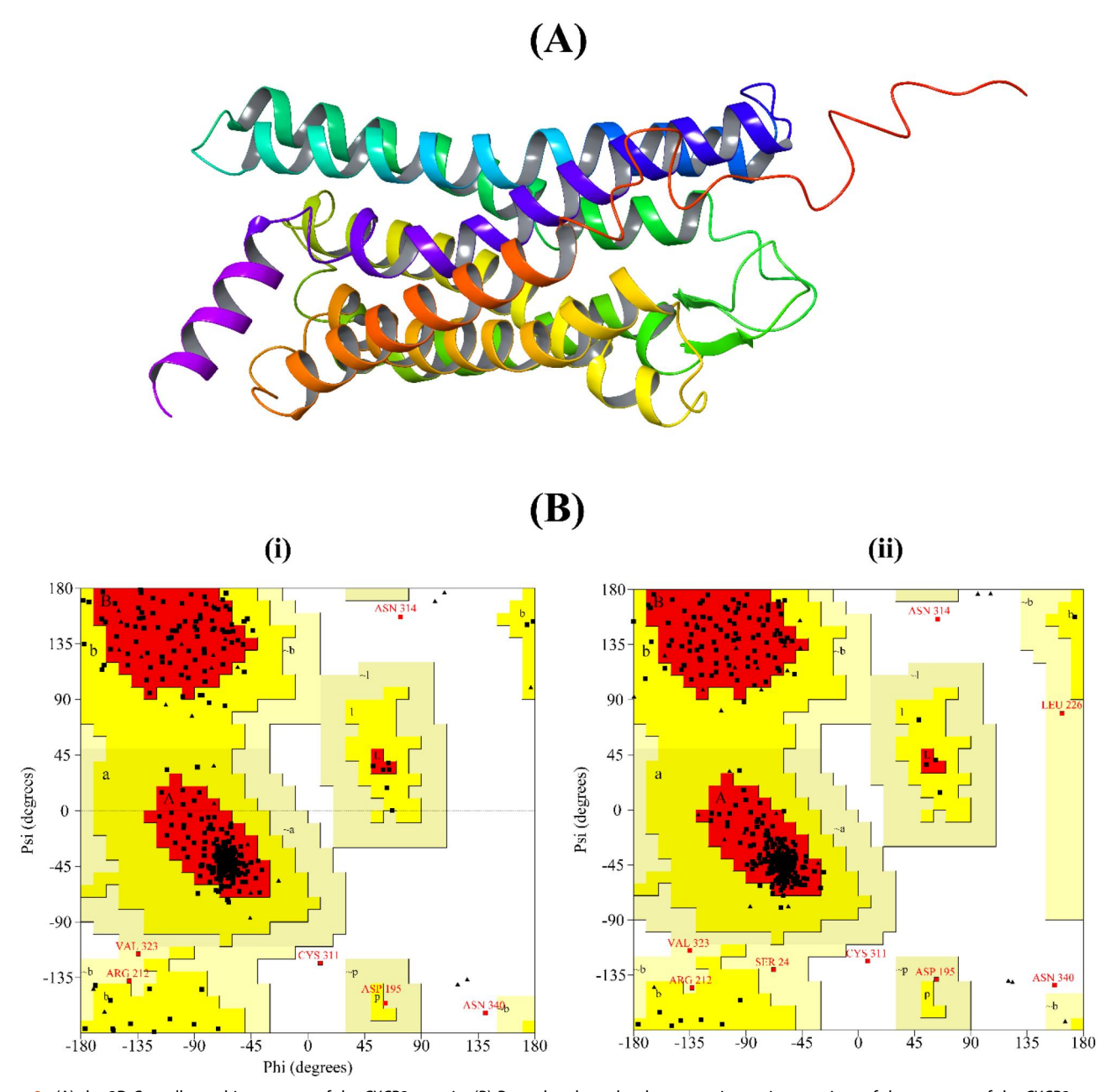


Figure 9. (A) the 3D Crystallographic structure of the CXCR3 protein. (B) Ramachandran plot demonstrating various sections of the structure of the CXCR3 receptor protein (i) and CXCR3-imatinib complex (ii). Here, the red-marked area indicates the most favoured regions for the residues, the yellow zone denotes the additional allowed regions, and the glycine residues are plotted as triangles.

imatinib was finally evaluated through DFT, molecular dynamics simulation, PCA, DCCM, and MM-GBSA calculations as the top-most drug candidate

0.148 eV (Figure 11). Furthermore, the hardness and softness energy of imatinib was 0.074 and 13.514 eV. Table 6 shows the results of the DFT calculation for imatinib.

3.9. Ligand optimization by density functional theory

Frontier molecular orbitals, namely the Highest Occupied Molecular Orbital (HOMO) and Lowest Unoccupied Molecular Orbital (LUMO), are of paramount significance in characterizing the reactivity and stability of ligand-receptor interactions for chemical species (Jana & Singh, 2019). In this study, we employed density functional theory (DFT) to computationally determine the orbital energies of imatinib. According to the DFT results, the HOMO and LUMO energy scores were -0.200 and -0.052 a.u, where the energy gap (HLG) was

3.10. Molecular dynamics simulation

The molecular dynamics study was conducted to analyze the structural variations and rigidity of the docked complex in a simulating environment. The root mean square deviations of the C-alpha atoms of the simulating systems were illustrated in Figure 12 where the Apo (CXCR3 receptor protein) and the docked complex (imatinib-CXCR3) had an initial increase in RMSD due to the flexible behavior of the complex. Both protein systems were stabilized after 20 ns and maintained a lower degree of the deviations till the whole simulations

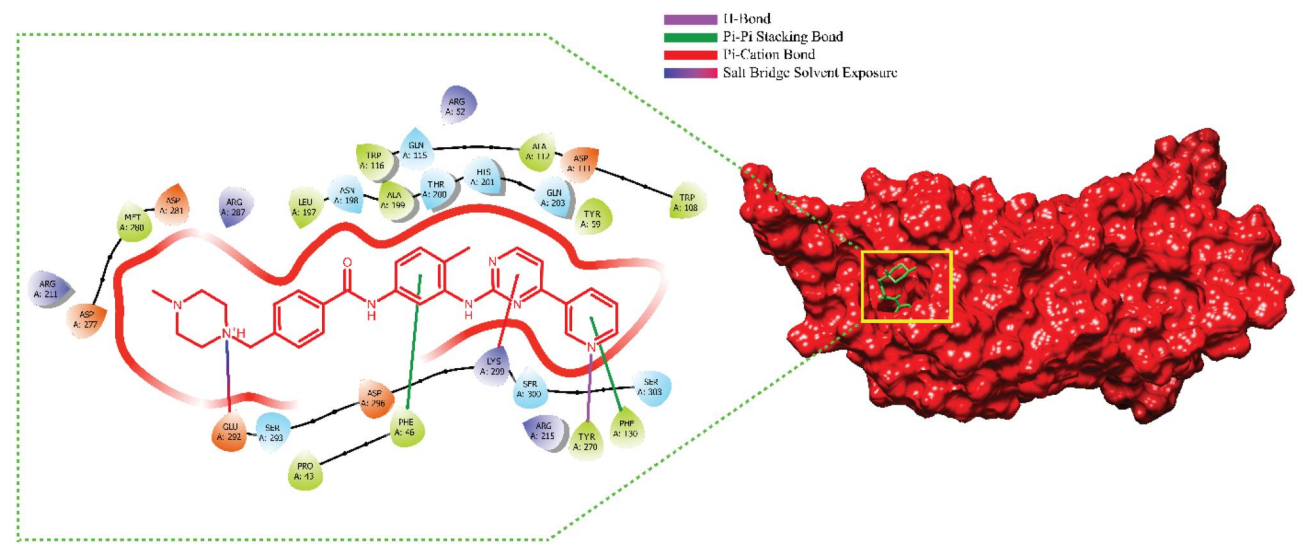


Figure 10. The molecular interaction between imatinib and the CXCR3 chemokine receptor through molecular docking study.

Table 5. The top 10 drug molecules with their binding affinity and MM-GBSA scores (Kcal/mol) with the CXCR3 receptor.

Drug molecules	Binding affinity (kcal/mol)	MM-GBSA scores (dG _{bind}) (kcal/mol	
Imatinib	-7.338	-68.27	
Lycorine	-7.092	-45.93	
3-Nitrofluoranthene	-6.702	-44.32	
Cicloheximide	-6.061	-43.45	
Irinotecan	-5.592	-55.56	
Rolipram	-5.465	-40.67	
Roflumilast	-5.129	-35.27	
Gadodiamide hydrate	-4.683	-19.73	
Roxarsone	-3.732	-20.69	
Thapsigargin	-1.585	-48.10	

times. The RMSD profile of both systems did not exceed 3 Å, defining the stable nature of the complex.

The root mean square fluctuation of protein systems is a benchmark that defines flexibility across the regions (Hasib et al., 2022). Figure 13 indicates that the RMSF value of the CXCR3 protein and the imatinib-CXCR3 complex was lower than 2.5 Å which denotes the conformational stability of both complexes. The CXCR3-imatinib complex showed less fluctuation during simulation compared to Apo (CXCR3 receptor). The majority of the variation occurred at the beginning and end of the MD simulation as the N- and C-terminal domains were present.

Moreover, the solvent accessible surface area is a key determinant of protein stability. The higher SASA indicates an expansion in the protein structure, whereas the lower SASA defines the truncated nature of the complexes. Figure 14 showed that the protein complex had an initial rise in SASA at the start of the simulation but reached stable states after 40 ns. The CXCR3-imatinib complex maintained a stable profile during the rest of the simulation periods, which correlates with the compactness of the system.

Similarly, the compactness of protein is determined by the radius of gyration (Rg). The Rg value defines the distribution of atoms across a protein-ligand complex. The lower radius of gyration indicates tight packing of protein in a simulating system (Lobanov et al., 2008). In the Rg analysis, the CXCR3-imatinib complex exhibited almost a flat line throughout the simulation, indicating the structural compactness of the system (Figure 15).

In addition, the intramolecular interaction formed by different bonds between the CXCR3 receptor and imatinib was analyzed. The intramolecular hydrogen bond of the complex defines the stability and rigidity of the protein system. Figure 16 indicates that imatinib interacted with CXCR3 by forming several bonds, such as the hydrogen, hydrophobic, ionic, and water bridges, and maintained these contacts throughout the simulation period. In addition, we have calculated the PSA and molSA values for the CXCR3-imatinib complex where the complex showed stability during simulation (See Supplementary File 3)

Principal component analysis (PCA) has been widely used to analyze the dynamic behavior of proteins (David & Jacobs, 2014). It enables the identification of collective motions exhibited by protein trajectories during molecular dynamics (MD) simulations. In our study, we employed PCA to analyze the CXCR3-imatinib complex system (Figure 17(A)), plotting the eigenvalues against their corresponding eigenvector indices for the first 20 modes of motion. These eigenvalues represent fluctuations in the protein's eigenvectors within hyperspace. In particular, the overall movement of the proteins in our simulations is primarily governed by eigenvectors with higher eigenvalues. Among the first five eigenvectors, which displayed dominant movements, eigenvalues ranging from 18.3% to 80.2% were observed, while the remaining eigenvectors exhibited lower eigenvalues.

To capture the majority of total variations, we focused on the first three principal components, PC1, PC2, and PC3,

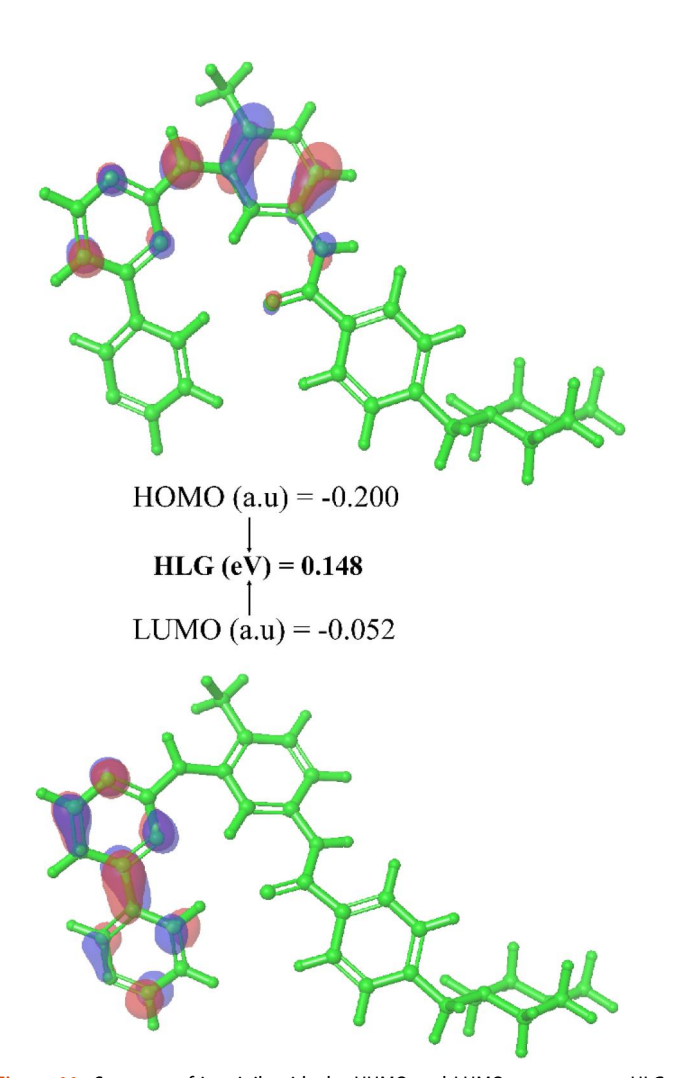


Figure 11. Structure of imatinib with the HUMO and LUMO energy score. HLG represents the energy gap between HUMO and LUMO.

which collectively accounted for over 40% of the total variability. Analyzing Figure 17(A), we observed that PC1 demonstrated the highest variability, accounting for 18.26% of the overall motion, followed by PC2 with a variability of 13.02%. On the contrary, PC3 exhibited minimal variability at 11.54%. This reduced variability indicates that PC3 corresponds to a stabilized protein-ligand binding state, occupies a relatively confined region in phase space and adopts a compact structure compared to PC1 and PC2. Using simple clustering within the PC subspace, our PCA analysis successfully uncovered conformational changes across all clusters. Blue regions exhibited the most significant movement, white regions demonstrated intermediate movement, while red regions suggested reduced flexibility and movement.

Furthermore, the pairwise correlation map, depicted in Figure 17(B), provided insights into the relationship between imatinib and the CXCR3 protein. The map displayed pairwise cross-correlation coefficients, with values above 0.8 representing strong positive correlations and highlighted in cyan. Conversely, residues with anticorrelated behavior, indicated by values below -0.4, were marked in purple. The high percentage of pairwise-correlated residues signifies a stable binding between the CXCR3 receptor protein and imatinib, thus confirming their strong interaction.

3.11. Binding free energy calculation

The MM-GBSA approach is commonly employed for assessing the binding free energy between protein molecules and ligands. In this study, we investigated the impact of various non-bonded interaction energies on the binding free energy of the CXCR3-imatinib complex. Our findings revealed that the binding free energy of imatinib to CXCR3 was determined to be -83.66 kcal/mol (Figure 18). Among the

Table 6. Density functional theory calculation result of imatinib after molecular docking and MM-GBSA analysis.

Compound name	PubChem ID	εHOMO (a.u)	εLUMO (a.u)	HLG (eV)	(Hardness (eV)	Softness (eV)
lmatinib	CID-5291	-0.200	-0.052	0.148	0.074	13.514

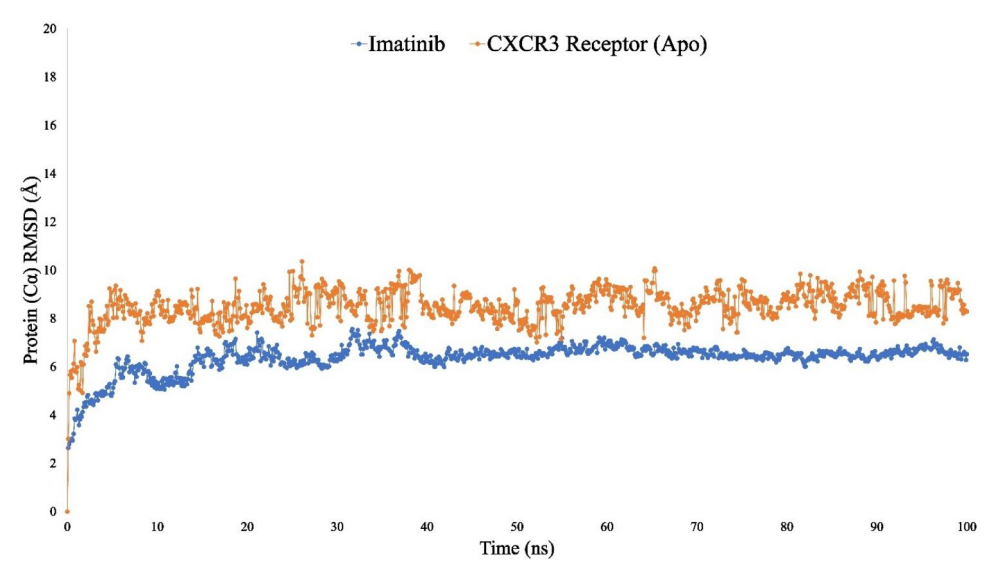


Figure 12. Molecular dynamics simulation trajectory analysis to determine the conformational stability of CXCR3 after the binding of imatinib through the calculation of RMSD values.

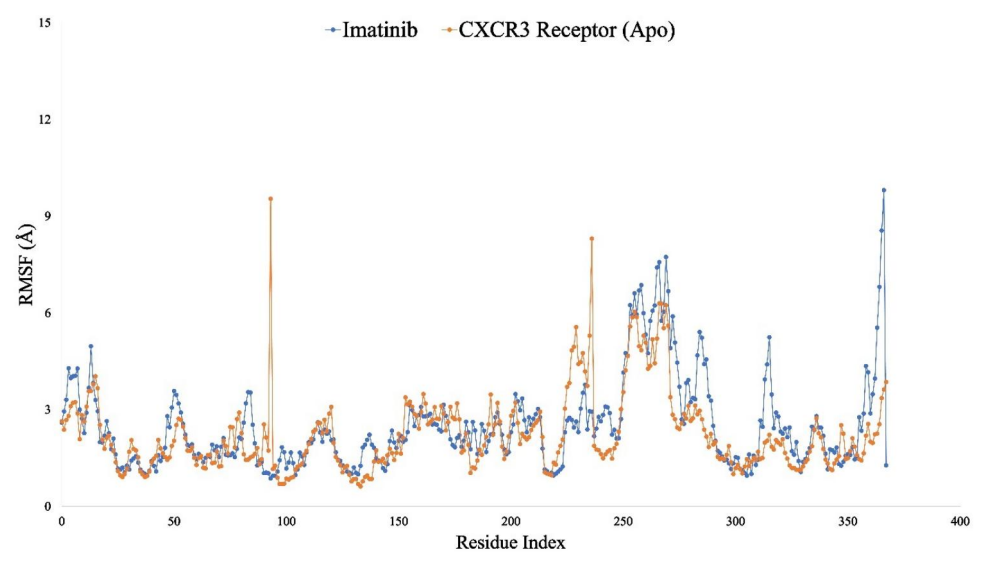


Figure 13. Determination of the RMSF value for the protein C atoms in the docked CXCR3-imatinib complex.

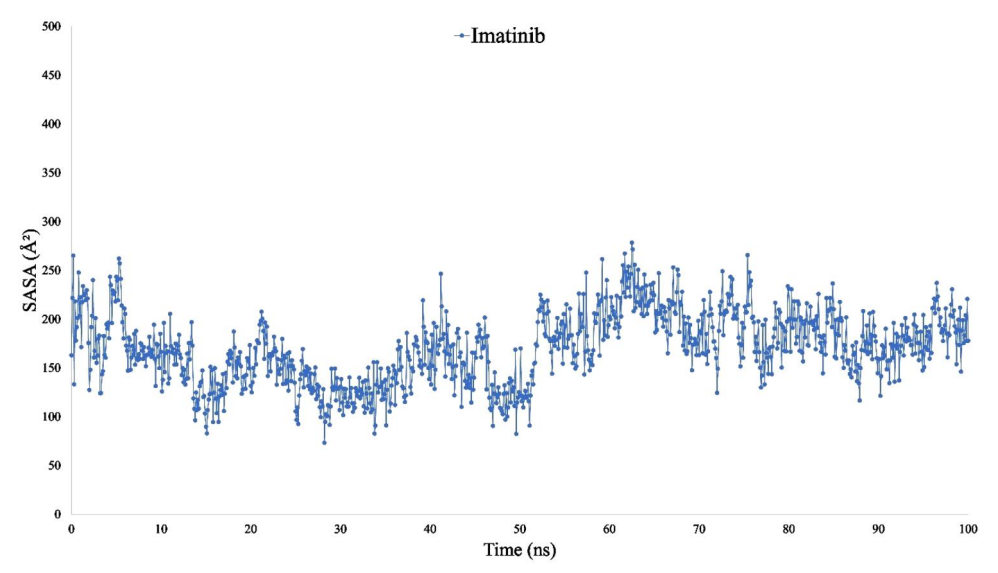


Figure 14. Calculation of the solvent accessible surface area (SASA) value for the selected ligand and CXCR3 receptor using 100 ns simulation.

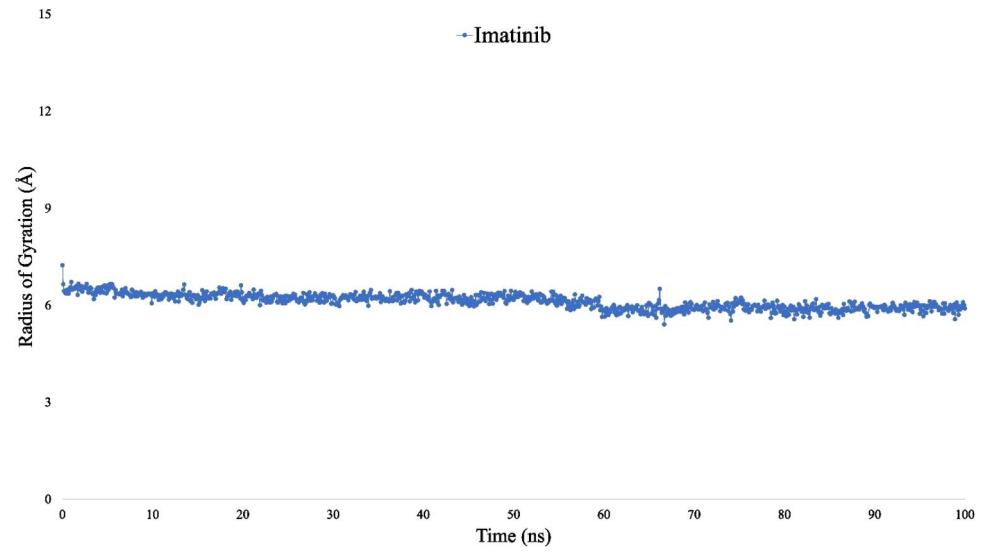


Figure 15. Radius of gyration (Rg) analysis for the CXCR3-imatinib complex by employing 100 ns molecular dynamics simulation.

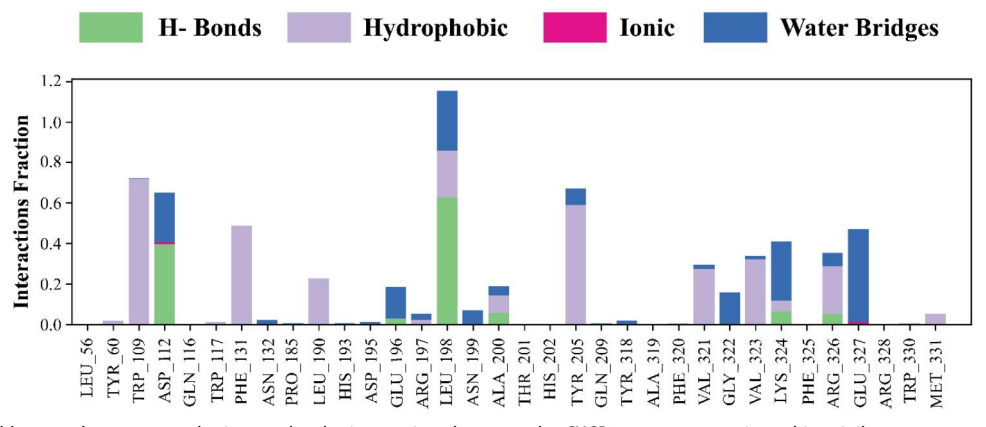


Figure 16. The stacked bar graphs represent the intramolecular interactions between the CXCR3 receptor protein and imatinib.

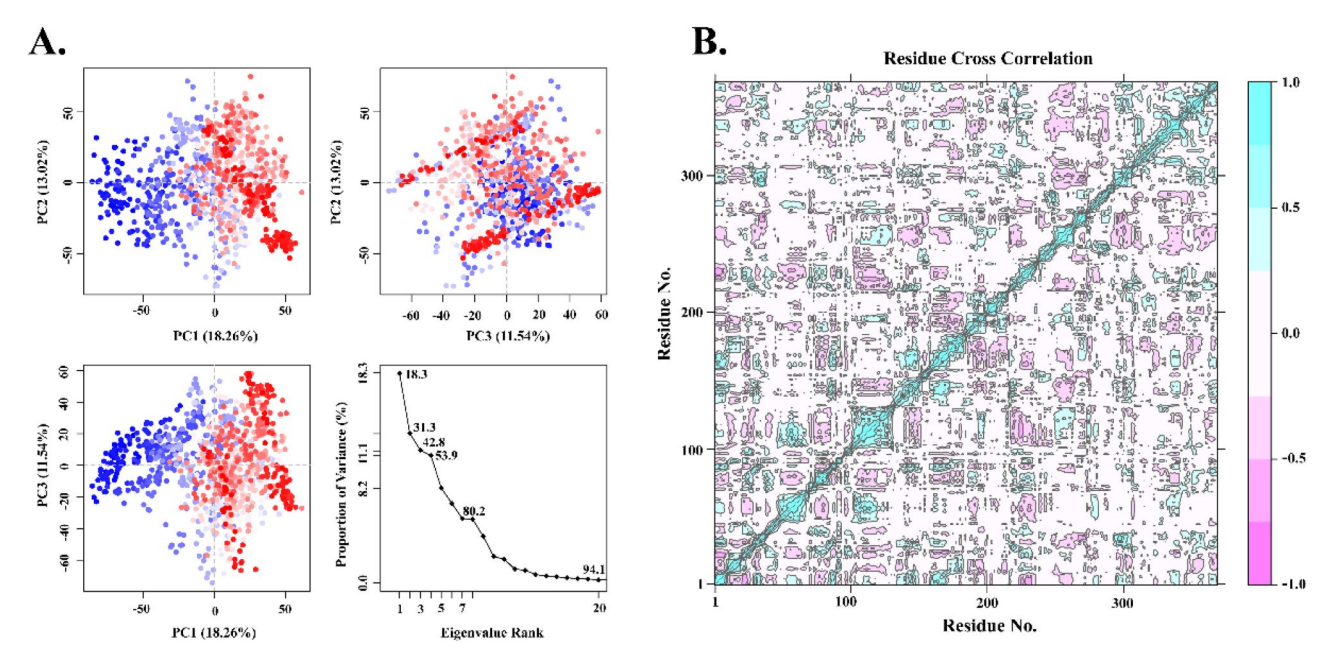


Figure 17. (A) Principal component analysis for the CXCR3-imatinib complex. Here, the eigenvalue was plotted against the proportion of variance (%). three PCs represent the areas of fluctuations. The variations in PC1, PC2, and PC3 were 18.26%, 13.02%, and 11.54%, respectively. The overall rate of variation was 42.82%. (B) The dynamic cross-correlation mapping of the CXCR3-imatinib complex exhibits positive and negative correlations among the constituent residues. The positive correlation between residues is denoted by cyan color and the negative correlation is indicated by purple color.

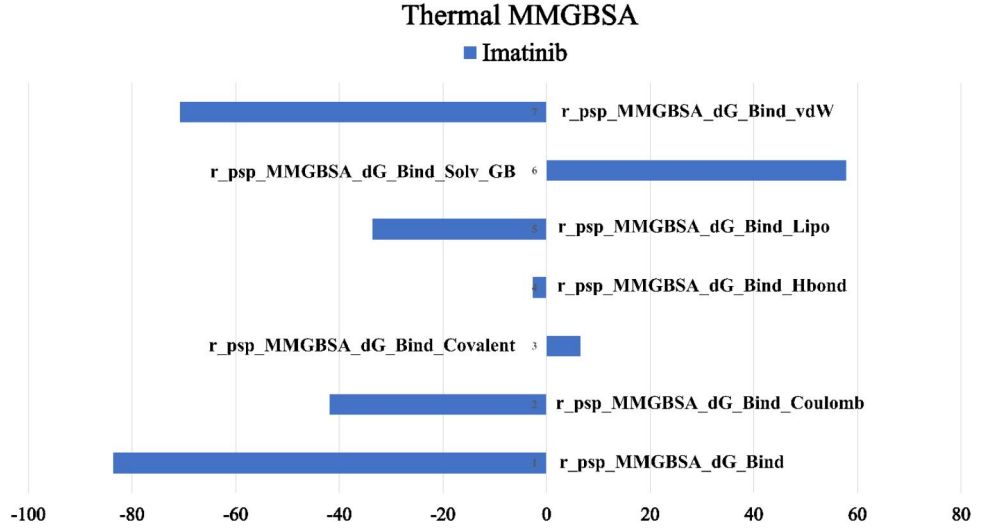


Figure 18. Representation of the average binding free MM-GBSA energy and other energy parameters for the CXCR3-imatinib complex.

Table 7. The average MM-GBSA binding free energy calculation of imatinib with CXCR3 from post molecular dynamics simulation trajectories.

Parameters	Energies (Kcal/mol)
dG _{bind}	-83.66
dG _{bind} Coulomb	-41.84
dG _{bind} Covalent	6.50
dG _{bind} Hbond	-2.71
dG _{bind} Lipo	-33.59
dG _{bind} SolvGB	57.86
dG _{bind} vdW	-70.74

different types of interactions, the GbindvdW, GbindLipo, GbindCoulomb, and GbindSolvGB energies exerted the most significant influence on the average binding energy. Conversely, the contribution of the GbindCovalent energy to the overall binding energy was found to be minimal. Furthermore, the interaction analysis based on GbindHbond values demonstrated the formation of stable hydrogen bonds between the CXCR3-imatinib complex. Table 7 showed the binding free energy and other non-bonded interaction energies for the CXCR3-imatinib complex.

4. Discussion

The majority of cases of impairment are triggered by neurological disorders, which are also the second leading cause of death worldwide. Especially in low and middle-income countries, the actual numbers of deaths and individuals with disabilities caused by neurological disorders have increased significantly in the last 30 years (Feigin et al., 2020). Many nervous system disorders are minimally responsive to existing treatments, but are potential candidates for gene therapy, an approach that can correct the genetic abnormalities contributing to its pathogenesis at the molecular level (Choong et al., 2016). Keeping this part in memory, we analyzed the differential gene expression pattern for two significant neurological disorders, namely Guillain-Barré syndrome (GBS) and autism spectrum disorder (ASD), to identify potential candidate biomarkers for therapeutic purposes. Guillain-Barré syndrome (GBS) is an autoimmune disorder that affects the peripheral nervous system and is associated with a wide range of comorbidities, including rapidly evolving muscle weakness, a lack of myotatic reflexes, moderate sensory loss, and areflexia (Dimachkie & Barohn, 2013; Wang et al., 2016). Besides, autism spectrum disorder is also a neurological disorder characterized by persistent deficits in social communication and interactions (Brown et al., 2017; Cryan et al., 2020). Despite having great clinical value, the interconnection between GBS and ASD remains a mystery. Hence, we have used several bioinformatics approaches to evaluate the expression patterns of significant DEGs and their pathways related to GBS and ASD, which can be impactful therapeutic targets for these two disorders. The remaining study was completed with the analysis of PPIs, hub genes identification and module interpretation, TF-gene interactions, TF-miRNA coregulatory network, and candidate drug detection. Furthermore, we performed molecular docking, MM-GBSA, DFT, molecular dynamics simulation, PCA, and DCCM approaches to interpret the potency of the identified drug candidates.

We studied two RNA-seq gene expression datasets (GSE72748 and GSE113834) from GEO-NCBI and detected 693 and 365 DEGs respectively. To predict the connections and probable drug compounds for GBS and ASD, 17 common DEGs were identified. Following that, related GO terms and pathways were identified according to the lower pvalue using these 17 DEGs. In terms of GO biological processes, positive regulation of cAMP-mediated signaling, regulation of cAMP metabolic process, positive regulation of purine nucleotide, and positive regulation of cyclic nucleotide are the topmost GO terms. One of the most vital elements for neuronal expansion, plasticity, and regeneration is cAMP. Members of the cAMP-dependent second-messenger pathways have a role in cellular proliferation and differentiation, as well as embryonic development, especially neurodevelopment (Blaschke et al., 2000). Notably, protein kinase A (PKA) is triggered by cAMP, and various studies have suggested that proteins involved in the PKA pathway may be linked to autism (Ji et al., 2011). Also, in a previous study, it was claimed that, for therapeutic interventions, molecular components that participate in cAMP-mediated signaling pathways can serve as appealing drug targets due to their contribution as a second messenger in the central nervous system (Lee, 2015).

The top GO terms for molecular function are CXCR chemokine receptor binding, chemokine activity, chemokine receptor binding, and cytokine activity. MIF (Macrophage migration inhibitory factor) signaling is activated after binding of the chemokine receptors, CXCR2, CXCR4, and CXCR7 (Jankauskas et al., 2019). MIF has been studied as a neuroendocrine mediator and plays a pro-inflammatory role in various immunoinflammatory and autoimmune conditions such as type 1 diabetes, multiple sclerosis, Guillain-Barré syndrome, and different types of cancers, including neuroblastoma (Benedek et al., 2017; Cavalli et al., 2019; Cvetkovic et al., 2005; Fagone et al., 2018; Kasama et al., 2010; Leyton-Jaimes et al., 2018; Mangano et al., 2018; Nicoletti et al., 2005; Presti et al., 2018; Soumoy et al., 2019). The synthesis of CXCRs was found to change in ASD patients in several investigations. The gene expression of the CXCR2, CXCR3, CXCR5 and CXCR7 receptors was found to be higher in patients with ASD (Ahmad et al., 2018). Furthermore, the top GO terms according to the cellular component are collagencontaining extracellular matrix, secretory granule lumen, and tertiary granule lumen. To date, no evidence of these cellular components playing a role in GBS or ASD has been reported.

The relevant KEGG, WikiPathways, and Bioplanet pathways for GBS and ASD were then determined. The research was carried out using common DEGs to uncover pathways that were identical in both GBS and ASD. Viral protein interaction with cytokine and cytokine receptor, Cytokine-cytokine receptor interaction, and chemokine signaling pathway are the major KEGG pathways identified in the current study. Chemokines appear to be a special type of neurotransmitter that control a wide range of biological processes, including neural development, neuroinflammation, and synaptic transmission (Rostène et al., 2011). Chemokine receptor signaling elements may offer novel therapeutic options for children

with autism spectrum disorder and other neurological impairments because the chemokine signaling pathway has been reported to be involved in the peripheral and central nervous system (Ahmad et al., 2018; Uboqu, 2013). Meanwhile, the chemokine signaling pathway, type II interferon signaling, and toll-like receptor signaling pathway were identified as top WikiPathways. Type II interferon (IFNy) contributes to neurodegeneration in a variety of CNS disorders; however, its particular role in CNS inflammation is not fully understood (Kulkarni et al., 2016). In earlier investigations, toll-like receptors are involved in several diseases of the central nervous system, such as Alzheimer's and multiple sclerosis (Carty & Bowie, 2011). In the BioPlanet pathway analysis, binding of chemokines to chemokine receptors, cytokinecytokine receptor interaction, TWEAK regulation of gene expression, and chemokine signaling pathway were found to be the supreme pathways. According to recent studies, suppression of TWEAK expression in the CNS has therapeutic benefits in patients with multiple sclerosis and ischemic stroke (Nagy et al., 2021).

The most important part of the investigation is the construction and exploration of the PPIs network, which is integral for hub gene identification, module analysis, and probable drug prediction. The 17 common DEGs underwent the PPI analysis to build the network. The PPI network designated CCL5, CCL18, CXCL12, CXCL1, CXCL8, CCL2, CXCL9, CXCL10, CXCL2, and CCL3 genes as hub genes due to their high interaction rate. Furthermore, essential modules based on the PPI network were also identified because these dense areas reveal valuable insights into the molecular nature of different types of disorders (Vlaic et al., 2018). Among the common DEGs, CXCL9, CXCL10 and PF4 were found in the module analysis, while the CXCL9 and CXCL10 genes are also the identified hub genes. Previously, CXCL10 was elevated in the CSF of patients with GBS or CIDP, while a reduced concentration of CXCL9 and CXCL10 was also reported in other studies. These previous findings validate the relevance of the current study.

Following that, we also identified some transcriptional factors that are essential for the functions of these common DEGs. The pathogenicity of various human diseases like neurodegenerative disorders and ischemic damage is related to the uncontrolled expression of these transcriptional regulators (Kane & Citron, 2009). Likewise, transcriptional factors contribute to a variety of biological processes, and the abnormal activity of these TFs may be promising therapeutic targets (Papavassiliou & Papavassiliou, 2016). In the TF-gene interaction network, TNXB was regulated by the highest number of TF-genes with a degree value of 57. Here, CXCL10 and CXCL9 also exhibited a notable interaction. The degree values of CXCL10 and CXCL9 were 9 and 6, respectively, in our TF-gene network. Evidence from the literature reveals that, under physiological and pathological conditions, CXCL9, CXCL10, and CXCL11, together with their receptors, play a pivotal role in the central nervous system (Koper et al., 2018).

Furthermore, the coregulatory network of miRNAs and TFs was constructed, as these regulatory molecules act as

potential biomarkers in different complex disorders. To date, an increasing number of miRNAs have been shown to be critical for the pathogenesis of neurological diseases (Nudelman et al., 2010). The expression of miRNAs is altered in conjunction with the onset and progression of disorders in the central nervous system. Therefore, miRNA-mediated regulation could play a significant role in the initiation and progression of neurological disorders and may serve as a new biomarker (Wang et al., 2014). A total of 85 miRNAs were identified in this study. Among miRNAs, miR-135, miR-135b, and miR-186 were connected to CXCL9 and CXCL10 in the coregulatory network and were found to have roles in neurological disorders in earlier studies (Che et al., 2014; Samadian et al., 2021; Yang et al., 2018). Both miR-135, miR-135b, and miR-186 previously showed a negative regulatory effect on the expression and activity of BACE-1 and thus play a significant role in the progression of Alzheimer's disease because BACE-1 is a key drug target for AD (Kim et al., 2016; Liu et al., 2014; Zhang et al., 2016). miR-135b played a protective role in Parkinson's disease by inhibiting pyroptosis by targeting FoxO1 (Zeng et al., 2019). Although the direct connection between the identified miRNAs and GBS or ASD is not proven yet but their role in other neurological disorders denotes their ability to work as potential biomarkers in GBS and ASD.

Next, probable drug candidates for GBS and ASD were identified from the DSigDB database utilizing the 17 common DEGs. Here, we highlighted the top 10 drug candidates (Table 4) where gadodiamide hydrate CTD 00002623, imatinib CTD 00003267, and cicloheximide PC3 UP were identified as the top candidates based on their lower pvalue.

Then, the top 10 drug candidates went through molecular docking analysis to dictate their efficacy. Candidates were docked with the chemokine receptor CXCR3. The chemokine receptor CXCR3 is activated by the chemokines CXCL9, CXCL10, and CXCL11 (Andrews & Cox, 2016; Schmidt et al., 2015), and previous studies have shown that CXCL9, 10, and 11 all bind to CXCR3 (Campanella et al., 2008; Müller et al., 2010). In this study, both CXCL9 and CXCL10 were identified as hub gene and essential module, and also most of the drug molecules interacted with them. Hence, we choose the CXCR3 receptor to implement the molecular docking analysis with the candidate drug molecules. Imatinib exhibited the highest binding affinity score of -7.338 kcal/mol in the molecular docking study. Imatinib interacted with the amino acid residues TYR-270, PHE-46,130, GLU-292 and LYS-299 of the CXCR3 protein by forming different types of bonds. Although there is no information in the literature linking these amino acid residues directly with GBS and ASD, the relevance of this research is indicated by their roles in neurotransmission and neuroprotection (Cheng et al., 2020; Crupi et al., 2019; Kolacheva et al., 2022). In addition, we calculated the MM-GBSA score to predict the binding free energy of the docked complexes where imatinib showed the highest dGbind score of -68.27 kcal/mol. Studies have shown the role of imatinib in modulating the pathophysiological state of a number of disorders affecting the brain and spinal cord, such as Alzheimer's disease, Parkinson's disease, stroke,

multiple sclerosis, and spinal cord injury (Kumar et al., 2019). The density functional theory calculation was also employed as it determine the pharmacological properties of small molecules (Bouback et al., 2021). We calculated the HOMO, LUMO, and their energy gap values. A greater energy difference is always expected for small compounds to become bioactive (Zhan et al., 2003). In this study, the HOMO-LUMO values and the energy gap between them indicate the bioactive properties of imatinib.

To further our investigation, we conducted molecular dynamics (MD) simulations to ascertain the structural stability of the imatinib-CXCR3 receptor complex. The root mean square deviation (RMSD) and root mean square fluctuation (RMSF) values of the complex remained below 3 Å, indicating the stability of the complex. Furthermore, the complex demonstrated a consistent conformation in terms of radius of gyration (Rg), solvent accessible surface area (SASA), and intramolecular interaction bond analysis. Over the course of the 100 ns simulations, the CXCR3-imatinib complex exhibited minimal fluctuations, confirming the compactness of the system. The reliability of the MD simulations was further corroborated by employing principal component analysis (PCA) and dynamic cross-correlation map (DCCM) analysis. PCA results revealed limited variations, while DCCM analysis exhibited a strong correlation between CXCR3 and imatinib, affirming the validity of MD simulations. Finally, the determination of the binding free energy (MM-GBSA) was carried out based on the analysis of post MD simulation trajectories. Notably, a substantial increase in net negative binding free energy (-83.66 kcal/mol) was observed following the simulation of the CXCR3-imatinib complex. This observed enhancement in binding free energy serves as compelling evidence, highlighting the congruence between the binding free energy derived from molecular docking data and the MM-GBSA values obtained from the MD simulation trajectories.

In summary, the current study attempted to uncover the interconnection between GBS and ASD through different bioinformatic approaches. Identified pathways and gene ontological pathways using common DEGs were found to interact with hub genes, especially with CXCL9 and CXCL10. CXCL9 and CXCL10 were prioritized over the other hub genes due to their presence in the module analysis and their roles in various neurological disorders according to earlier studies. Furthermore, identified TFs and miRNAs that are connected to CXCL9 and CXCL10 were previously found to have roles in brain disorders. Among the drug molecules, imatinib exhibited the best binding affinity and MM-GBSA score with the CXCR3 receptor and remained stable throughout the simulation process. Imatinib interacted with the hub genes CXCL9 and CXCL10 in the drug candidate identification process via the DSigDB database. The findings of this network-based study demonstrated a discernible correlation between the hub genes CXCL9 and CXCL10 and all observed outcomes, thereby establishing the relevance of this research endeavor. Hopefully, the biomarkers identified in this study may provide significant insights into the pathophysiology of GBS and ASD, and the identified drug molecules may show a treatment path for these two brain disorders. At the same time, this study does not have clinical validation. Therefore, further laboratory-based research is highly recommended for clinical validation.

5. Conclusion

Despite recent advancement of science and biological research, the definite link between GBS and ASD has not established yet. Hence we evaluated the differential expression pattern of genes from two RNA-seg data to discover potential biomarkers and drug candidates for GBS and ASD. The present study identified several relevant pathways, such as the cAMP-mediated signaling pathway, the chemokine signaling pathway, and the toll-like receptor signaling pathway, that had been somewhat related to neurological disorders before. A total of ten hub genes were identified in the current investigation, where CXCL9 and CXCL10 were also found in the module analysis. The rest of the analysis was performed by predicting the subsequent TFs, miRNAs, and target drug molecules. Among the drug molecules, imatinib exhibited the highest binding affinity and MM-GBSA score with the CXCR3 receptor. In addition, the complexes remained stable during the molecular dynamics simulation and fluctuated less. The results of MD Simulations were further validated by PCA and DCCM analysis supporting the potential of imatinib as a treatment option for GBS and ASD. We tried to put a spotlight on the mysterious relationship between GBS and ASD throughout the study. Although this study may help to identify some potential biomarkers and drug candidates for GBS and ASD, further laboratory research is necessary for clinical validation.

Acknowledgments

We express our gratitude to all of our well-wishers for their everlasting encouragement and support.

Disclosure statement

The authors declare no conflict of interest.

Funding

The author(s) reported that there is no funding associated with the work featured in this article.

Authors' contributions

RAH and MCA designed the whole project. RAH, SA, SS, SZS, and ZA wrote the manuscript. RAH and MHR did the analysis and made the figures. MSSS performed the molecular dynamics simulation. MHR and MAHMJ reviewed and supervised the entire project.

References

Ahmad, S. F., Ansari, M. A., Nadeem, A., Bakheet, S. A., Al-Ayadhi, L. Y., & Attia, S. M. (2018). Upregulation of peripheral CXC and CC chemokine receptor expression on CD4(+) T cells is associated with immune



- dysregulation in children with autism. Progress in Neuro-Psychopharmacology & Biological Psychiatry, 81, 211-220. https://doi. org/10.1016/j.pnpbp.2017.10.001
- Anaya, J.-M., Rodríguez, Y., Monsalve, D. M., Vega, D., Ojeda, E., González-Bravo, D., Rodríguez-Jiménez, M., Pinto-Díaz, C. A., Chaparro, P., Gunturiz, M. L., Ansari, A. A., Gershwin, M. E., Molano-González, N., Ramírez-Santana, C., & Acosta-Ampudia, Y. (2017). A comprehensive analysis and immunobiology of autoimmune neurological syndromes during the Zika virus outbreak in Cucuta, Colombia. Journal of Autoimmunity, 77, 123-138. https://doi.org/10.1016/j.jaut.2016.12.007
- Andrews, S. P., & Cox, R. J. (2016). Small-molecule CXCR3 antagonists. Journal of Medicinal Chemistry, 59(7), 2894–2917. https://doi.org/10. 1021/acs.imedchem.5b01337
- Ansar, V., & Valadi, N. (2015). Guillain-Barré syndrome. Primary Care, 42(2), 189-193. https://doi.org/10.1016/j.pop.2015.01.001
- Athanasios, A., Charalampos, V., Vasileios, T., & Ashraf, G. M. (2017). Protein-protein interaction (PPI) network: Recent advances in drug discovery. Current Drug Metabolism, 18(1), 5-10. https://doi.org/10. 2174/138920021801170119204832
- Ayub, U., Haider, I., & Naveed, H. (2020). SAlign-a structure-aware method for global PPI network alignment. BMC Bioinformatics, 21(1), 500. https://doi.org/10.1186/s12859-020-03827-5
- Bae, J. S., Yuki, N., Kuwabara, S., Kim, J. K., Vucic, S., Lin, C. S., & Kiernan, M. C. (2014). Guillain-Barré syndrome in Asia. Journal of Neurology, Neurosurgery, and Psychiatry, 85(8), 907-913. https://doi.org/10.1136/ jnnp-2013-306212
- Barrett, T., Wilhite, S. E., Ledoux, P., Evangelista, C., Kim, I. F., Tomashevsky, M., Marshall, K. A., Phillippy, K. H., Sherman, P. M., Holko, M., Yefanov, A., Lee, H., Zhang, N., Robertson, C. L., Serova, N., Davis, S., & Soboleva, A. (2012). NCBI GEO: Archive for functional genomics data sets-update. Nucleic Acids Research, 41(D1), D991-D995. https://doi.org/10.1093/nar/gks1193
- Barzegar, M., Rouhi, A. H. J., Farhoudi, M., & Sardashti, S. (2012). A report of a probable case of familial Guillain-Barre syndrome. Annals of Indian Academy of Neurology, 15(4), 299-302. https://doi.org/10.4103/ 0972-2327.104341
- Benedek, G., Meza-Romero, R., Jordan, K., Zhang, Y., Nguyen, H., Kent, G., Li, J., Siu, E., Frazer, J., Piecychna, M., Du, X., Sreih, A., Leng, L., Wiedrick, J., Caillier, S. J., Offner, H., Oksenberg, J. R., Yadav, V., Bourdette, D., Bucala, R., & Vandenbark, A. A. (2017). MIF and D-DT are potential disease severity modifiers in male MS subjects. Proceedings of the National Academy of Sciences of the United States of America. 114(40), E8421-E8429. https://doi.org/10.1073/pnas. 1712288114
- Benjamini, Y., & Hochberg, Y. (1995). Controlling the false discovery rate: A practical and powerful approach to multiple testing. Journal of the Royal Statistical Society: Series B (Methodological), 57(1), 289-300. https://doi.org/10.1111/j.2517-6161.1995.tb02031.x
- Berciano, J., Sedano, M. J., Pelayo-Negro, A. L., García, A., Orizaola, P., Gallardo, E., Lafarga, M., Berciano, M. T., & Jacobs, B. C. (2017). Proximal nerve lesions in early Guillain-Barré syndrome: Implications for pathogenesis and disease classification. Journal of Neurology, 264(2), 221-236. https://doi.org/10.1007/s00415-016-8204-2
- Bhandari, R., Paliwal, J. K., & Kuhad, A. (2020). Neuropsychopathology of autism spectrum disorders: Complex interplay of genetic, epigenetic, and environmental factors. Advances in Neurobiology, 24, 97-141.
- Biswas, P., Dey, D., Rahman, A., Islam, M. A., Susmi, T. F., Kaium, M. A., Hasan, M. N., Rahman, M. D. H., Mahmud, S., Saleh, M. A., Paul, P., Rahman, M. R., Al Saber, M., Song, H., Rahman, M. A., & Kim, B. (2021). Analysis of the SYK gene as a prognostic biomarker and suggested potential bioactive phytochemicals as an alternative therapeutic option for colorectal cancer: An in silico pharmaco-informatics investigation. Journal of Personalized Medicine, 11(9), 888. https://doi.org/10. 3390/ipm11090888
- Blaschke, R. J., Monaghan, A. P., Bock, D., & Rappold, G. A. (2000). A novel murine PKA-related protein kinase involved in neuronal differentiation. Genomics, 64(2), 187-194. https://doi.org/10.1006/geno.
- Blum, S., Csurhes, P., Reddel, S., Spies, J., & McCombe, P. (2014). Killer immunoglobulin-like receptor and its HLA ligands in Guillain-Barre

- syndrome. Journal of Neuroimmunology, 267(1-2), 92-96. https://doi. org/10.1016/j.jneuroim.2013.12.007
- Blum, S., Ji, Y., Pennisi, D., Li, Z., Leo, P., McCombe, P., & Brown, M. A. (2018). Genome-wide association study in Guillain-Barre syndrome. Journal of Neuroimmunology, 323, 109-114. https://doi.org/10.1016/j. ineuroim 2018.07.016
- Bochevarov, A. D., Harder, E., Hughes, T. F., Greenwood, J. R., Braden, D. A., Philipp, D. M., Rinaldo, D., Halls, M. D., Zhang, J., & Friesner, R. A. (2013). Jaguar: A high-performance quantum chemistry software program with strengths in life and materials sciences. International Journal of Quantum Chemistry, 113(18), 2110-2142. https://doi.org/10. 1002/qua.24481
- Bouback, T. A., Pokhrel, S., Albeshri, A., Aljohani, A. M., Samad, A., Alam, R., Hossen, M. S., Al-Ghamdi, K., Talukder, M. E. K., Ahammad, F., Qadri, I., & Simal-Gandara, J. (2021). Virtual screening based on pharmacophores, quantum mechanic calculations and molecular dynamics simulation approaches identified potential candidates for natural antiviral drugs against MERS-CoV S1-NTD. Molecules (Basel, Switzerland), 26(16), 4961. https://doi.org/10.3390/molecules26164961
- Brown, J. T., Eum, S., Cook, E. H., & Bishop, J. R. (2017). Pharmacogenomics of autism spectrum disorder. Pharmacogenomics. 18(4), 403-414. https://doi.org/10.2217/pgs-2016-0167
- Campanella, G. S. V., Tager, A. M., El Khoury, J. K., Thomas, S. Y., Abrazinski, T. A., Manice, L. A., Colvin, R. A., & Luster, A. D. (2008). Chemokine receptor CXCR3 and its ligands CXCL9 and CXCL10 are required for the development of murine cerebral malaria. Proceedings of the National Academy of Sciences of the United States of America, 105(12), 4814-4819. https://doi.org/10.1073/pnas.0801544105
- Cao, D. D., Li, L., & Chan, W. Y. (2016). MicroRNAs: Key regulators in the central nervous system and their implication in neurological diseases. International Journal of Molecular Science, 17(6), 842.
- Carty, M., & Bowie, A. G. (2011). Evaluating the role of toll-like receptors in central nervous system. Biochemical Pharmacology, 81(7), 825-837. https://doi.org/10.1016/j.bcp.2011.01.003
- Cavalli, E., Mazzon, E., Basile, M. S., Mangano, K., Di Marco, R., Bramanti, P., Nicoletti, F., Fagone, P., & Petralia, M. C. (2019). Upregulated expression of macrophage migration inhibitory factor, its analogue Ddopachrome tautomerase and the CD44 receptor in peripheral CD4 T cells from clinically isolated syndrome patients with rapid conversion to clinically defined multiple sclerosis. Medicina, 55(10), 667. https:// doi.org/10.3390/medicina55100667
- Chang, K.-H., Chuang, T.-J., Lyu, R.-K., Ro, L.-S., Wu, Y.-R., Chang, H.-S., Huang, C.-C., Kuo, H.-C., Hsu, W.-C., Chu, C.-C., & Chen, C.-M. (2012). Identification of gene networks and pathways associated with Guillain-Barré syndrome. PloS One, 7(1), e29506. https://doi.org/10. 1371/journal.pone.0029506
- Che, H., Sun, L.-H., Guo, F., Niu, H.-F., Su, X.-L., Bao, Y.-N., Fu, Z. D., Liu, H.-L., Hou, X., Yang, B.-F., & Ai, J. (2014). Expression of amyloid-associated miRNAs in both the forebrain cortex and the hippocampus of middle-aged rats. Cellular Physiology and Biochemistry: International Journal of Experimental Cellular Physiology, Biochemistry, Pharmacology, 33(1), 11-22. https://doi.org/10.1159/000356646
- Chen, E. Y., Tan, C. M., Kou, Y., Duan, Q., Wang, Z., Meirelles, G. V., Clark, N. R., & Ma'ayan, A. (2013). Enrichr: Interactive and collaborative HTML5 gene list enrichment analysis tool. BMC Bioinformatics, 14(1), 128. https://doi.org/10.1186/1471-2105-14-128
- Chen, S.-H., Chin, C.-H., Wu, H.-H., Ho, C.-W., Ko, M.-T., & Lin, C.-Y.. cyto-Hubba: A Cytoscape plug-in for hub object analysis in network biology [Paper presentation]. 20th International Conference on Genome Informatics, Citeseer.
- Cheng, C., Alexander, R., Min, R., Leng, J., Yip, K. Y., Rozowsky, J., Yan, K.-K., Dong, X., Djebali, S., Ruan, Y., Davis, C. A., Carninci, P., Lassman, T., Gingeras, T. R., Guigó, R., Birney, E., Weng, Z., Snyder, M., & Gerstein, M. (2012). Understanding transcriptional regulation through integrative analysis of transcription factor binding data. Genome Research, 22(9), 1658-1667. https://doi.org/10.1101/gr.136838.111
- Cheng, J., Tang, J.-C., Pan, M.-X., Chen, S.-F., Zhao, D., Zhang, Y., Liao, H.-B., Zhuang, Y., Lei, R.-X., Wang, S., Liu, A.-C., Chen, J., Zhang, Z.-H., Li, H.-T., Wan, Q., & Chen, Q.-X. (2020). I-lysine confers neuroprotection by suppressing the inflammatory response through microRNA-



- 575/PTEN signaling after mouse intracerebral hemorrhage injury. Experimental Neurology, 327, 113214. https://doi.org/10.1016/j. expneurol.2020.113214
- Chin, C.-H., Chen, S.-H., Wu, H.-H., Ho, C.-W., Ko, M.-T., & Lin, C.-Y. (2014). cytoHubba: Identifying hub objects and subnetworks from complex interactome. BMC Systems Biology, 8s(Suppl 4), S11. https://doi.org/10. 1186/1752-0509-8-S4-S11
- Choong, C. J., Baba, K., & Mochizuki, H. (2016). Gene therapy for neurological disorders. Expert Opinion on Biological Therapy, 16(2), 143–159. https://doi.org/10.1517/14712598.2016.1114096
- Christensen, D. L., Bilder, D. A., Zahorodny, W., Pettygrove, S., Durkin, M. S., Fitzgerald, R. T., Rice, C., Kurzius-Spencer, M., Baio, J., & Yeargin-Allsopp, M. (2016). Prevalence and characteristics of autism spectrum disorder among 4-year-old children in the autism and developmental disabilities monitoring network. Journal of Developmental and Behavioral Pediatrics: JDBP, 37(1), 1-8. https://doi.org/10.1097/DBP. 0000000000000235
- Crupi, R., Impellizzeri, D., & Cuzzocrea, S. (2019). Role of metabotropic glutamate receptors in neurological disorders. Frontiers in Molecular Neuroscience, 12, 20. https://doi.org/10.3389/fnmol.2019.00020
- Cryan, J. F., O'Riordan, K. J., Sandhu, K., Peterson, V., & Dinan, T. G. (2020). The gut microbiome in neurological disorders. The Lancet. Neurology, 19(2), 179–194. https://doi.org/10.1016/S1474-4422(19)
- Cvetkovic, I., Al-Abed, Y., Miljkovic, D., Maksimovic-Ivanic, D., Roth, J., Bacher, M., Lan, H. Y., Nicoletti, F., & Stosic-Grujicic, S. (2005). Critical role of macrophage migration inhibitory factor activity in experimental autoimmune diabetes. Endocrinology, 146(7), 2942-2951. https:// doi.org/10.1210/en.2004-1393
- Dash, S., Pai, A. R., Kamath, U., & Rao, P. (2015). Pathophysiology and diagnosis of Guillain-Barré syndrome - Challenges and needs. International Journal of Neuroscience, 125(4), 235-240. https://doi.org/ 10.3109/00207454.2014.913588
- David, C. C., & Jacobs, D. J. (2014). Principal component analysis: A method for determining the essential dynamics of proteins. Methods in Molecular Biology (Clifton, N.J.), 1084, 193–226. https://doi.org/10. 1007/978-1-62703-658-0_11
- De Las Rivas, J., & Fontanillo, C. (2010). Essentials of protein-protein interactions: Key concepts to building and analyzing interactome networks. PLoS Computational Biology, 6(6), e1000807. https://doi.org/10. 1371/journal.pcbi.1000807
- Dimachkie, M. M., & Barohn, R. J. (2013). Guillain-Barré syndrome and variants. Neurologic Clinics, 31(2), 491-510. https://doi.org/10.1016/j. ncl.2013.01.005
- Doms, A., & Schroeder, M. (2005). GoPubMed: Exploring PubMed with the gene ontology. Nucleic Acids Research, 33(Web Server issue), W783-786. https://doi.org/10.1093/nar/gki470
- Doncel-Pérez, E., Mateos-Hernández, L., Pareja, E., García-Forcada, Á., Villar, M., Tobes, R., Romero Ganuza, F., Vila Del Sol, V., Ramos, R., Fernández de Mera, I. G., & de la Fuente, J. (2016). Expression of the early growth response gene-2 and regulated cytokines correlates with recovery from Guillain-Barré syndrome. Journal of Immunology (Baltimore, Md.: 1950), 196(3), 1102-1107. https://doi.org/10.4049/jimmunol.1502100
- Fagone, P., Mazzon, E., Cavalli, E., Bramanti, A., Petralia, M. C., Mangano, K., Al-Abed, Y., Bramati, P., & Nicoletti, F. (2018). Contribution of the macrophage migration inhibitory factor superfamily of cytokines in the pathogenesis of preclinical and human multiple sclerosis: In silico and in vivo evidence. Journal of Neuroimmunology, 322, 46-56. https://doi.org/10.1016/j.jneuroim.2018.06.009
- Feigin, V. L., Vos, T., Nichols, E., Owolabi, M. O., Carroll, W. M., Dichgans, M., Deuschl, G., Parmar, P., Brainin, M., & Murray, C. (2020). The global burden of neurological disorders: Translating evidence into policy. Lancet. Neurology, 19(3), 255-265. https://doi.org/10.1016/S1474-4422(19)30411-9
- Ferreira, L. G., Dos Santos, R. N., Oliva, G., & Andricopulo, A. D. (2015). Molecular coupling and structure-based drug design strategies. Molecules (Basel, Switzerland), 20(7), 13384-13421. https://doi.org/10. 3390/molecules200713384

- Fujimura, H. (2013). The Guillain-Barré syndrome. Handbook of Clinical Neurology, 115, 383-402.
- Genheden, S., & Ryde, U. (2015). The MM/PBSA and MM/GBSA methods to estimate ligand-binding affinities. Expert Opinion on Drug Discovery, 10(5), 449-461. https://doi.org/10.1517/17460441.2015.1032936
- Harrach, M. F., & Drossel, B. (2014). Structure and dynamics of TIP3P, TIP4P, and TIP5P water near smooth and atomistic walls of different hydroaffinities. Journal of Chemical Physics. 140, 174501.
- Hasib, R. A., Ali, M. C., Rahman, M. S., Rahman, M. M., Ahmed, F. F., Mashud, M. A. A., Islam, M. A., & Jamal, M. A. H. M. (2022). A computational biology approach for the identification of potential SARS-CoV-2 main protease inhibitors from natural essential oil compounds. F1000Research, 10, 1313. https://doi.org/10.12688/f1000research. 73999.2
- Heikema, A. P., Islam, Z., Horst-Kreft, D., Huizinga, R., Jacobs, B. C., Wagenaar, J. A., Poly, F., Guerry, P., van Belkum, A., Parker, C. T., & Endtz, H. P. (2015). Campylobacter jejuni capsular genotypes are related to Guillain-Barré syndrome. Clinical Microbiology and Infection, 21(9), e851-852-852.e9. https://doi.org/10.1016/j.cmi.2015.05.031
- Holmans, P., Green, E. K., Pahwa, J. S., Ferreira, M. A. R., Purcell, S. M., Sklar, P., Owen, M. J., O'Donovan, M. C., & Craddock, N, Wellcome Trust Case-Control Consortium. (2009). Analysis of the gene ontology of GWA study data sets provides insights into the biology of bipolar disorder. American Journal of Human Genetics, 85(1), 13-24. https:// doi.org/10.1016/j.ajhg.2009.05.011
- Huang, R., Grishagin, I., Wang, Y., Zhao, T., Greene, J., Obenauer, J. C., Ngan, D., Nguyen, D.-T., Guha, R., Jadhav, A., Southall, N., Simeonov, A., & Austin, C. P. (2019). The NCATS BioPlanet - An integrated platform to explore the universe of cellular signaling pathways for toxicology, systems biology, and chemical genomics. Frontiers in Pharmacology, 10, 445. https://doi.org/10.3389/fphar.2019.00445
- Jacobson, M. P., Pincus, D. L., Rapp, C. S., Day, T. J. F., Honig, B., Shaw, D. E., & Friesner, R. A. (2004). A hierarchical approach to all-atom protein loop prediction. Proteins, 55(2), 351-367. https://doi.org/10.1002/ prot.10613
- Jana, S., & Singh, S. K. (2019). Identification of selective MMP-9 inhibitors through multiple e-pharmacophore, ligand-based pharmacophore, molecular coupling, and density functional theory approaches. Journal of Biomolecular Structure & Dynamics, 37(4), 944-965. https:// doi.org/10.1080/07391102.2018.1444510
- Jankauskas, S. S., Wong, D. W. L., Bucala, R., Djudjaj, S., & Boor, P. (2019). Evolving complexity of MIF signaling. Cellular Signalling, 57, 76-88. https://doi.org/10.1016/j.cellsig.2019.01.006
- Ji, L., Chauhan, V., Flory, M. J., & Chauhan, A. (2011). Brain region-specific decrease in protein kinase A activity and expression in the frontal cortex of regressive autism. PloS One, 6(8), e23751. https://doi.org/10. 1371/journal.pone.0023751
- Jussila, K., Junttila, M., Kielinen, M., Ebeling, H., Joskitt, L., Moilanen, I., & Mattila, M.-L. (2020). Sensory abnormality and quantitative autism traits in children with and without autism spectrum disorder in an epidemiological population. Journal of Autism and Developmental Disorders, 50(1), 180–188. https://doi.org/10.1007/s10803-019-04237-0
- Kandeel, M., Igbal, M. N., Ali, I., Malik, S., Malik, A., & Sehgal, S. A. (2023). Comprehensive in silico analyses of flavonoids elucidating the drug properties against kidney disease by targeting AIM2. PloS One, 18(5), e0285965. https://doi.org/10.1371/journal.pone.0285965
- Kane, M. J., & Citron, B. A. (2009). Transcription factors as therapeutic targets in CNS disorders. Recent Patents on CNS Drug Discovery, 4(3), 190-199. https://doi.org/10.2174/157488909789104820
- Kanehisa, M., Goto, S., Sato, Y., Furumichi, M., & Tanabe, M. (2012). KEGG for the integration and interpretation of large-scale molecular data sets. Nucleic Acids Research, 40(Database issue), D109-114. https://doi. org/10.1093/nar/gkr988
- Kasama, T., Ohtsuka, K., Sato, M., Takahashi, R., Wakabayashi, K., & Kobayashi, K. (2010). Macrophage migration inhibitory factor: A multifunctional cytokine in rheumatic diseases. Arthritis, 2010, 106202-106210. https://doi.org/10.1155/2010/106202
- Kim, J., Yoon, H., Chung, D.-E., Brown, J. L., Belmonte, K. C., & Kim, J. (2016). Chung De et al. miR 186 is decreased in aged brain and

- suppresses BACE 1 expression. Journal of Neurochemistry, 137(3), 436-445. https://doi.org/10.1111/jnc.13507
- Kim, Y. S., Leventhal, B. L., Koh, Y.-J., Fombonne, E., Laska, E., Lim, E.-C., Cheon, K.-A., Kim, S.-J., Kim, Y.-K., Lee, H., Song, D.-H., & Grinker, R. R. (2011). Prevalence of autism spectrum disorders in a total population sample. American Journal of Psychiatry, 168(9), 904-912. https://doi. org/10.1176/appi.ajp.2011.10101532
- Kolacheva, A., Alekperova, L., Pavlova, E., Bannikova, A., & Ugrumov, M. V. (2022). Changes in tyrosine hydroxylase activity and dopamine synthesis in the nigrostriatal system of mice in an acute model of Parkinson's disease as a manifestation of neurodegeneration and neuroplasticity. Brain Sciences, 12(6), 779. https://doi.org/10.3390/ brainsci12060779
- Koper, O. M., Kamińska, J., Sawicki, K., & Kemona, H. (2018). CXCL9, CXCL10, CXCL11 and their receptor (CXCR3) in neuroinflammation and neurodegeneration. Advances in Clinical and Experimental Medicine: Official Organ Wroclaw Medical University, 27(6), 849-856. https://doi.org/10.17219/acem/68846
- Kuleshov, M. V., Jones, M. R., Rouillard, A. D., Fernandez, N. F., Duan, Q., Wang, Z., Koplev, S., Jenkins, S. L., Jagodnik, K. M., Lachmann, A., McDermott, M. G., Monteiro, C. D., Gundersen, G. W., & Ma'ayan, A. (2016). Enrichr: A comprehensive gene set enrichment analysis web server 2016 update. Nucleic Acids Research, 44(W1), W90-97. https:// doi.org/10.1093/nar/gkw377
- Kulkarni, A., Ganesan, P., & O'Donnell, L. A. (2016). Interferon gamma: Influence on neural stem cell function in neurodegenerative and neuroinflammatory diseases. Clinical Medical Insights: Pathology, 9, 9–19.
- Kumar, M., Kulshrestha, R., Singh, N., & Jaggi, A. S. (2019). Expanding the spectrum of the anticancer drug, imatinib, in disorders affecting brain and spinal cord. Pharmacological Research, 143, 86-96. https://doi.org/ 10.1016/j.phrs.2019.03.014
- Laskowski, R., MacArthur, M., & Thornton, J. (2006). PROCHECK: Validation of protein structure coordinates.
- Lee, D. (2015). Global and local missions of cAMP signaling in neural plasticity, learning, and memory. Frontiers in Pharmacology, 6, 161. https://doi.org/10.3389/fphar.2015.00161
- Leonhard, S. E., Mandarakas, M. R., Gondim, F. A. A., Bateman, K., Ferreira, M. L. B., Cornblath, D. R., van Doorn, P. A., Dourado, M. E., Hughes, R. A. C., Islam, B., Kusunoki, S., Pardo, C. A., Reisin, R., Sejvar, J. J., Shahrizaila, N., Soares, C., Umapathi, T., Wang, Y., Yiu, E. M., Willison, H. J., & Jacobs, B. C. (2019). Diagnosis and treatment of Guillain-Barré syndrome in ten steps. Nature Reviews. Neurology, 15(11), 671-683. https://doi.org/10.1038/s41582-019-0250-9
- Leyton-Jaimes, M. F., Kahn, J., & Israelson, A. (2018). Macrophage migration inhibitory factor: A multifaceted cytokine implicated in multiple neurological diseases. Experimental Neurology, 301(Pt B), 83-91. https://doi.org/10.1016/j.expneurol.2017.06.021
- Li, J., Abel, R., Zhu, K., Cao, Y., Zhao, S., & Friesner, R. A. (2011). The VSGB 2.0 model: A next-generation energy model for high-resolution protein structure modeling. Proteins, 79(10), 2794-2812. https://doi.org/ 10.1002/prot.23106
- Li, M., Wu, X., Wang, J., & Pan, Y. (2012). Towards the identification of protein complexes and functional modules by integrating PPI network and gene expression data. BMC Bioinformatics, 13(1), 109. https://doi. org/10.1186/1471-2105-13-109
- Liu, C.-G., Wang, J.-L., Li, L., Xue, L.-X., Zhang, Y.-Q., & Wang, P.-C. (2014). MicroRNA-135a and-200b, potential biomarkers for Alzheimer's disease, regulate β secretase and amyloid precursor protein. Brain Research, 1583, 55-64. https://doi.org/10.1016/j.brainres.2014.04.026
- Liu, Y., Chen, T.-Y., Yang, Z.-Y., Fang, W., Wu, Q., & Zhang, C. (2020). Identification of central genes in papillary thyroid carcinoma: Robust rank aggregation and weighted gene coexpression network analysis. Journal of Translational Medicine, 18(1), 170. https://doi.org/10.1186/ s12967-020-02327-7
- Liu, Z.-P., Wu, C., Miao, H., & Wu, H. (2015). RegNetwork: An integrated database of transcriptional and post-transcriptional regulatory networks in humans and mouse. Database: The Journal of Biological Databases and Curation, 2015, bav095. https://doi.org/10.1093/database/bav095

- Lobanov, M., Bogatyreva, N. S., & Galzitskaia, O. V. [(2008). Radius of gyration is an indicator of compactness of protein structure. Molekuliarnaia Biologiia, 42(4), 701-706. https://doi.org/10.1134/ S0026893308040195
- Lord, C., Brugha, T. S., Charman, T., Cusack, J., Dumas, G., Frazier, T., Jones, E. J. H., Jones, R. M., Pickles, A., State, M. W., Taylor, J. L., & Veenstra-VanderWeele, J. (2020). Autism spectrum disorder. Nature Reviews. Disease Primers, 6(1), 5. https://doi.org/10.1038/s41572-019-0138-4
- Love, M. I., Huber, W., & Anders, S. (2014). Moderated estimation of fold change and dispersion for RNA-seq data with DESeq2. Genome Biology, 15(12), 550. https://doi.org/10.1186/s13059-014-0550-8
- Mangano, K., Mazzon, E., Basile, M. S., Di Marco, R., Bramanti, P., Mammana, S., Petralia, M. C., Fagone, P., & Nicoletti, F. (2018). Pathogenic role for macrophage migration inhibitory factor in glioblastoma and its targeting with specific inhibitors as a novel tailored therapeutic approach. Oncotarget, 9(25), 17951-17970. https://doi.org/ 10.18632/oncotarget.24885
- Manoli, D. S., & State, M. W. (2021). Autism spectrum disorder genetics and the search for pathological mechanisms. American Journal of Psychiatry, 178(1), 30-38. https://doi.org/10.1176/appi.ajp.2020. 20111608
- Miryala, S. K., Anbarasu, A., & Ramaiah, S. (2018). Discerning molecular interactions: A comprehensive review on biomolecular interaction databases and network analysis tools. Gene, 642, 84-94. https://doi. org/10.1016/j.gene.2017.11.028
- Mostafavi, M., & Gaitanis, J. (2020). Autism spectrum disorder and medical cannabis: Review and clinical experience. Seminars in Pediatric Neurology, 35, 100833. https://doi.org/10.1016/j.spen.2020.100833
- Müller, M., Carter, S., Hofer, M. J., & Campbell, I. L. (2010). The CXCR3 chemokine receptor and its ligands CXCL9, CXCL10 and CXCL11 in neuroimmunity - A story of conflict and conundrum. Neuropathology and Applied Neurobiology, 36(5), 368-387. https://doi.org/10.1111/j. 1365-2990.2010.01089.x
- Nagy, D., Ennis, K. A., Wei, R., Su, S. C., Hinckley, C. A., Gu, R.-F., Gao, B., Massol, R. H., Ehrenfels, C., Jandreski, L., Thomas, A. M., Nelson, A., Gyoneva, S., Hajós, M., & Burkly, L. C. (2021). The developmental synaptic regulator, TWEAK/Fn14 signaling, is a determinant of synaptic function in models of stroke and neurodegeneration. Proceedings of the National Academy of Sciences, 118(6), e2001679118. https://doi. org/10.1073/pnas.2001679118
- Negi, A., Shukla, A., Jaiswar, A., Shrinet, J., & Jasrotia, R. S. (2022. Applications and challenges of microarray and RNA-sequencing. Bioinformatics, 91-103.
- Nicoletti, F., Créange, A., Orlikowski, D., Bolgert, F., Mangano, K., Metz, C., Di Marco, R., & Al Abed, Y. (2005). Macrophage migration inhibitory factor (MIF) seems crucially involved in Guillain-Barre syndrome and experimental allergic neuritis. Journal of Neuroimmunology, 168(1-2), 168-174. https://doi.org/10.1016/j.jneuroim.2005.07.019
- Nisar, S., Bhat, A. A., Masoodi, T., Hashem, S., Akhtar, S., Ali, T. A., Amjad, S., Chawla, S., Bagga, P., Frenneaux, M. P., Reddy, R., Fakhro, K., & Haris, M. (2022). Genetics of glutamate and its receptors in autism spectrum disorder. Molecular Psychiatry, 27(5), 2380-2392. https://doi. org/10.1038/s41380-022-01506-w
- Nudelman, A. S., DiRocco, D. P., Lambert, T. J., Garelick, M. G., Le, J., Nathanson, N. M., & Storm, D. R. (2010). Neuronal activity rapidly induces the transcription of the CREB-regulated microRNA-132, in vivo. Hippocampus, 20(4), 492-498. https://doi.org/10.1002/hipo.
- Papavassiliou, K. A., & Papavassiliou, A. G. (2016). Transcription factor drug targets. Journal of Cellular Biochemistry, 117(12), 2693-2696. https://doi.org/10.1002/jcb.25605
- Parras, A., Anta, H., Santos-Galindo, M., Swarup, V., Elorza, A., Nieto-González, J. L., Picó, S., Hernández, I. H., Díaz-Hernández, J. I., Belloc, E., Rodolosse, A., Parikshak, N. N., Peñagarikano, O., Fernández-Chacón, R., Irimia, M., Navarro, P., Geschwind, D. H., Méndez, R., & Lucas, J. J. (2018). Autism-like phenotype and risk gene mRNA deadenylation by CPEB4 missplicing. Nature, 560(7719), 441-446. https://doi. org/10.1038/s41586-018-0423-5

- Pinzi, L., & Rastelli, G., 2019. Molecular docking: shifting paradigms in drug discovery. International journal of molecular sciences, 20(18),
- Podder, N. K., Rana, H. K., Azam, M. S., Rana, M. S., Akhtar, M. R., Rahman, M. R., Rahman, M. H., & Moni, M. A. (2020). A systemic biological approach to investigate the genetic profiling and comorbidities of type 2 diabetes. Gene Reports, 21, 100830. https://doi.org/10. 1016/i.genrep.2020.100830
- Presti, M., Mazzon, E., Basile, M. S., Petralia, M. C., Bramanti, A., Colletti, G., Bramanti, P., Nicoletti, F., & Fagone, P. (2018). Overexpression of macrophage migration inhibitory factor and functionally related genes, D-DT, CD74, CD44, CXCR2, and CXCR4, in glioblastoma. Oncology Letters, 16(3), 2881-2886. https://doi.org/10.3892/ol.2018.
- Rahman, M. H., Peng, S., Hu, X., Chen, C., Rahman, M. R., Uddin, S., Quinn, J. M. W. ... & Moni, M. A. (2020). A network-based bioinformatics approach to identify molecular biomarkers for type 2 diabetes that are linked to the progression of neurological diseases. International journal of environmental research and public health, 17(3), 1035.
- Roos, K., Wu, C., Damm, W., Reboul, M., Stevenson, J. M., Lu, C., Dahlgren, M. K., Mondal, S., Chen, W., Wang, L., Abel, R., Friesner, R. A., & Harder, E. D. (2019). OPLS3e: Extending force field coverage for drug-like small molecules. Journal of Chemical Theory and 15(3), 1863–1874. https://doi.org/10.1021/acs.jctc. Computation, 8b01026
- Rostène, W., Dansereau, M.-A., Godefroy, D., Van Steenwinckel, J., Reaux-Le Goazigo, A., Mélik-Parsadaniantz, S., Apartis, E., Hunot, S., Beaudet, N., & Sarret, P. (2011). Neurochemokines: A menage A three providing new insights on the functions of chemokines in the central nervous system. Journal of Neurochemistry, 118(5), 680-694. https://doi.org/10. 1111/i.1471-4159.2011.07371.x
- Safa, A., Azimi, T., Sayad, A., Taheri, M., & Ghafouri-Fard, S. (2021). A review of the role of genetic factors in Guillain-Barré syndrome. Journal of Molecular Neuroscience: MN, 71(5), 902-920. https://doi.org/ 10.1007/s12031-020-01720-7
- Samadian, M., Gholipour, M., Hajiesmaeili, M., Taheri, M., & Ghafouri-Fard, S. (2021). The eminent role of microRNAs in the pathogenesis of Alzheimer's disease. Frontiers in Aging Neuroscience, 13, 641080. https://doi.org/10.3389/fnagi.2021.641080
- Schmidt, D., Bernat, V., Brox, R., Tschammer, N., & Kolb, P. (2015). Identifying modulators of CXC receptors 3 and 4 with tailored selectivity using multitarget docking. ACS Chemical Biology, 10(3), 715-724. https://doi.org/10.1021/cb500577j
- Shahrizaila, N., Lehmann, H. C., & Kuwabara, S. (2021). Guillain-Barré syndrome. Lancet (London, England), 397(10280), 1214-1228. https://doi. org/10.1016/S0140-6736(21)00517-1
- Sharma, R., Jadhav, M., Choudhary, N., Kumar, A., Rauf, A., Gundamaraju, R., AlAsmari, A. F., Ali, N., Singla, R. K., Sharma, R., & Shen, B. (2022b). Deciphering the impact and mechanism of Trikatu, a spice-based formulation on alcoholic liver disease employing network pharmacology analysis and in vivo validation. Frontiers in Nutrition, 9, 1063118. https://doi.org/10.3389/fnut.2022.1063118
- Sharma, R., Singla, R. K., Banerjee, S., Sinha, B., Shen, B., & Sharma, R. (2022a). Role of Shankhpushpi (Convolvulus pluricaulis) in neurological disorders: An umbrella review covering evidence from ethnopharmacology to clinical studies. Neuroscience and Biobehavioral Reviews, 140, 104795. https://doi.org/10.1016/j.neubiorev.2022.104795
- Slenter, D. N., Kutmon, M., Hanspers, K., Riutta, A., Windsor, J., Nunes, N., Mélius, J., Cirillo, E., Coort, S. L., Digles, D., Ehrhart, F., Giesbertz, P., Kalafati, M., Martens, M., Miller, R., Nishida, K., Rieswijk, L., Waagmeester, A., Eijssen, L. M. T., ... Willighagen, E. L. (2018). WikiPathways: A multifaceted pathway database that combines metabolomics with other omics research. Nucleic Acids Research, 46(D1), D661-d667. https://doi.org/10.1093/nar/gkx1064
- Smoot, M. E., Ono, K., Ruscheinski, J., Wang, P.-L., & Ideker, T. (2011). Cytoscape 2.8: New features for data integration and network visualization. Bioinformatics (Oxford, England), 27(3), 431-432. https://doi. org/10.1093/bioinformatics/btq675

- Soumoy, L., Kindt, N., Ghanem, G., Saussez, S., & Journe, F. (2019). Role of macrophage migration inhibitory factor (MIF) in melanoma. Cancers, 11(4), 529. https://doi.org/10.3390/cancers11040529
- Taz, T. A., Ahmed, K., Paul, B. K., Kawsar, M., Aktar, N., Mahmud, S. M. H., & Moni, M. A. (2021). Network-based genetic identification effect of SARS-CoV-2 infections in patients with idiopathic pulmonary fibrosis (IPF). Briefings in Bioinformatics, 22(2), 1254-1266. https://doi.org/10. 1093/bib/bbaa235
- The Gene Ontology Consortium. (2017). Expanding the gene ontology knowledgebase and resources, Nucleic Acids Research, 45, D331-d338.
- Tilford, C. A., & Siemers, N. O. (2009). Gene set enrichment analysis. Methods in Molecular Biology, 563, 99-121.
- Ubogu, E. E. (2013). Chemokine-dependent signaling pathways in the peripheral nervous system. Methods in Molecular Biology (Clifton, N.J.), 1013. 17-30.
- Veenstra-VanderWeele, J., & Cook, E. H. Jr. (2004). Molecular genetics of autism spectrum disorder. Molecular Psychiatry, 9(9), 819-832. https:// doi.org/10.1038/sj.mp.4001505
- Vlaic, S., Conrad, T., Tokarski-Schnelle, C., Gustafsson, M., Dahmen, U., Guthke, R., & Schuster, S. (2018). ModuleDiscoverer: Identification of regulatory modules in protein-protein interaction networks. Scientific Reports, 8(1), 433. https://doi.org/10.1038/s41598-017-18370-2
- Wang, C., Ji, B., Cheng, B., Chen, J., & Bai, B. (2014). Neuroprotection of microRNAs in neurological disorders. Biomedical Reports, 2(5), 611-619. https://doi.org/10.3892/br.2014.297
- Wang, K., Li, M., & Bucan, M. (2007). Pathway-based approaches for analysis of genomewide association studies. American Journal of Human Genetics, 81(6), 1278-1283. https://doi.org/10.1086/522374
- Wang, Y., Liu, Z., Li, C., Li, D., Ouyang, Y., Yu, J., Guo, S., He, F., & Wang, W. (2012). Prediction of drug targets based on herbs components: The study on the multitarget pharmacological mechanism of qishenkeli acting on the coronary heart disease. Evidence-Based Complementary and Alternative Medicine, 2012, 1-10. https://doi.org/ 10 1155/2012/698531
- Wang, Y., Zhang, H.-L., Wu, X., & Zhu, J. (2016). Complications of Guillain-Barré syndrome. Expert Review of Clinical Immunology, 12(4), 439-448. https://doi.org/10.1586/1744666X.2016.1128829
- Wang, Z., Gerstein, M., & Snyder, M. (2009). RNA-Seq: A revolutionary tool for transcriptomics. Nature Reviews. Genetics, 10(1), 57-63. https:// doi.org/10.1038/nrg2484
- Warde-Farley, D., Donaldson, S. L., Comes, O., Zuberi, K., Badrawi, R., Chao, P., Franz, M., Grouios, C., Kazi, F., Lopes, C. T., Maitland, A., Mostafavi, S., Montojo, J., Shao, Q., Wright, G., Bader, G. D., & Morris, Q. (2010). The GeneMANIA prediction server: Biological network integration for gene prioritization and predicting gene function. Nucleic Acids Research, 38(Web Server issue), W214-W220. https://doi.org/10. 1093/nar/qkq537
- Webb, A. J. S., Brain, S. A. E., Wood, R., Rinaldi, S., & Turner, M. R. (2015). Seasonal variation in Guillain-Barré syndrome: A systematic review, meta-analysis, and Oxfordshire cohort study. Journal of Neurology, Neurosurgery, and Psychiatry, 86(11), 1196-1201. https://doi.org/10. 1136/innp-2014-309056
- Xia, J., Benner, M. J., & Hancock, R. E. (2014). NetworkAnalyst, integrative approaches for protein-protein interaction network analysis and visual exploration. Nucleic Acids Research, 42(Web Server issue), W167-174. https://doi.org/10.1093/nar/gku443
- Xia, J., Gill, E. E., & Hancock, R. E. (2015). NetworkAnalyst for statistical, visual, and network-based meta-analysis of gene expression data. Nature Protocols, 10(6), 823-844. https://doi.org/10.1038/nprot.2015.
- Yang, T. T., Liu, C. G., Gao, S. C., Zhang, Y., & Wang, P. C. (2018). The serum exosome derived MicroRNA- 135a,- 193b, and- 384 were potential Alzheimer's disease biomarkers. Biomedical Environmental Sciences, 31(2), 87-96.
- Yang, X., Kui, L., Tang, M., Li, D., Wei, K., Chen, W., Miao, J., & Dong, Y. (2020). High-throughput transcriptome profiling in drug and biomarker discovery. Frontiers in Genetics, 11, 19. https://doi.org/10.3389/ fgene.2020.00019



- Yeung, N., Cline, M. S., Kuchinsky, A., Smoot, M. E., & Bader, G. D. (2008). Exploring biological networks with Cytoscape software. Current Protocols in Bioinformatics, 23(1), 8-13.
- Yoo, M., Shin, J., Kim, J., Ryall, K. A., Lee, K., Lee, S., Jeon, M., Kang, J., & Tan, A. C. (2015). DSigDB: Drug signature database for gene set analysis. Bioinformatics (Oxford, England), 31(18), 3069-3071. https://doi. org/10.1093/bioinformatics/btv313
- Zablotsky, B., Black, L. I., & Blumberg, S. J. (2017). Estimated prevalence of children with diagnosed developmental disabilities in the United States, 2014-2016.
- Zeng, R., Luo, D.-X., Li, H.-P., Zhang, Q.-S., Lei, S.-S., & Chen, J.-H. (2019). MicroRNA-135b alleviates MPP + mediated Parkinson's disease in in vitro model by suppressing FoxO1-induced NLRP3 inflammasome and pyroptosis. Journal of Clinical Neuroscience: Official Journal of the Neurosurgical Society of Australasia, 65, 125-133. https://doi.org/10. 1016/j.jocn.2019.04.004
- Zhan C-G, Nichols JA, Dixon DA. Ionization potential, electron affinity, electronegativity, hardness, and electron excitation energy: Molecular properties from density functional theory orbital energies, Journal of Physical Chemistry A 2003;107:4184-4195. https://doi.org/10.1021/ jp0225774
- Zhang, H.-L., Zheng, X.-Y., & Zhu, J. (2013). Th1/Th2/Th17/Treg cytokines in Guillain-Barré syndrome and experimental autoimmune neuritis. Cytokine & Growth Factor Reviews, 24(5), 443-453. https://doi.org/10. 1016/j.cytogfr.2013.05.005
- Zhang, Y., Xing, H., Guo, S., Zheng, Z., Wang, H., & Xu, D. (2016). MicroRNA-135b has a neuroprotective role through targeting of β -site APP-cleaving enzyme 1. Experimental and Therapeutic Medicine, 12(2), 809-814. https://doi.org/10.3892/etm.2016.3366
- Zhou, G., Soufan, O., Ewald, J., Hancock, R. E. W., Basu, N., & Xia, J. (2019). NetworkAnalyst 3.0: A visual analytics platform for comprehensive gene expression profiling and meta-analysis. Nucleic Acids Research, 47(W1), W234-w241. https://doi.org/10.1093/nar/gkz240